Acta Numerica (2001), pp. 215–250 © Cambridge University Press, 2001

Some new results and current challenges in the finite element analysis of shells

Dominique Chapelle
INRIA-Rocquencourt, B.P. 105,
78153 Le Chesnay Cedex, France
E-mail: Dominique.Chapelle@inria.fr

This article, a companion to the article by Philippe G. Ciarlet on the mathematical modelling of shells also in this issue of *Acta Numerica*, focuses on numerical issues raised by the analysis of shells.

Finite element procedures are widely used in engineering practice to analyse the behaviour of shell structures. However, the concept of 'shell finite element' is still somewhat fuzzy, as it may correspond to very different ideas and techniques in various actual implementations. In particular, a significant distinction can be made between shell elements that are obtained via the discretization of shell models, and shell elements – such as the *general shell elements* – derived from 3D formulations using some kinematic assumptions, without the use of any shell theory. Our first objective in this paper is to give a unified perspective of these two families of shell elements. This is expected to be very useful as it paves the way for further thorough mathematical analyses of shell elements. A particularly important motivation for this is the understanding and treatment of the deficiencies associated with the analysis of *thin* shells (among which is the *locking* phenomenon). We then survey these deficiencies, in the framework of the *asymptotic behaviour* of shell models. We conclude the article by giving some detailed guidelines to numerically assess the performance of shell finite elements when faced with these pathological phenomena, which is essential for the design of improved procedures.

CONTENTS

1 Introduction 216
2 Two families of shell finite elements 219
3 Computational reliability issues for thin shells 226
References 247

https://doi.org/10.1017/S0962492901000034 Published online by Cambridge University Press

1. Introduction

Finite element procedures are widely used to analyse the behaviour of shell structures in various areas of engineering (*e.g.*, in the automotive, aerospace and civil engineering industries), and such analyses have been conducted ever since the early development of finite element methods. Over time, however, and across the various disciplines involved, the concept of 'shell finite element' has referred to very different ideas and techniques, and this situation has resulted in an incredibly abundant literature and in a significant amount of confusion. In this respect, we can identify in the 'zoology' of shell finite elements a particularly distinct 'line of division' between finite element methods that result from the discretization of shell mathematical models (namely, essentially two-dimensional models with unknowns given on the mid-surface of the shell; see, *e.g.*, Ciarlet (2000)) and finite element techniques obtained from various other – usually engineering-rooted – considerations. Roughly speaking, the finite element methods derived from a shell model draw their justification from the assumed relevance of such models, the solution of which they can be shown to approximate within a certain accuracy using numerical analysis techniques; see Bernadou (1996). By contrast, other shell finite element methods are grounded in mechanical considerations used 'at the element level'; see, for example, Bathe (1996) and the references therein. Although they are usually numerically tested using various benchmark problems, what is typically lacking for such finite element procedures is the proof that the finite element solutions converge to some known limit solution when the mesh is being refined. Indeed, the characterization of such a limit solution would be extremely useful for evaluating the whole approach.

One of the earliest techniques used in shell analysis consists in simply combining plate bending and membrane behaviour in flat elements, the collection of which approximates the geometry of the actual shell structure. This is known as the *facet-shell element* approach. Examples of this category of elements can be found in Batoz and Dhatt (1992). In Bernadou, Ducatel and Trouvé (1988), a basic facet-shell procedure is analysed and proved to be a non-conforming discretization scheme of a shell model. However, it is also shown that the corresponding consistency error is non-converging, and this result is consistent with previous observations of the lack of convergence exhibited by these methods; see, *e.g.*, Irons and Ahmad (1980). Additional deficiencies associated with the facet-type approximation of the geometry are identified in Akian and Sanchez-Palencia (1992). Various further refinements of the facet-shell techniques have been introduced, but whether or not these developments actually counteract the above-mentioned deficiencies is not clear (and indeed not proven). Moreover, by construction the coarse approximation of the geometry involved in these procedures implies that,

https://doi.org/10.1017/S0962492901000034 Published online by Cambridge University Press

even if a successfully converging scheme were to be found, the accuracy of the approximation would be rather poor.

On the other hand, shell finite element procedures obtained by directly discretizing a shell model can be thoroughly analysed and explicit error estimates are then obtained under some well-identified conditions (pertaining to the regularity of the exact solutions, the type of numerical integration used, *etc.*); see Bernadou (1996) and the references therein. The major drawback of this approach is, however, that building a shell finite element procedure on a *set shell model* is clearly restrictive as to the variety of situations that can be analysed. In particular, most shell theories are based on linear elastic behaviour, and adapting the models to account for an arbitrary three-dimensional (3D) constitutive equation – or for general nonlinear behaviour – is not straightforward. Note that this drawback in fact also applies to facet shell elements.

By contrast, a third methodology has been developed that specifically allows for unrestricted versatility as regards shell modelling capabilities. This methodology is based on the idea of 'degenerating' a 3D solid finite element into a shell element by using some *kinematic assumptions* for describing the variation of displacements across the thickness of the shell structure. Since the only model used is the 3D model in consideration, general 3D constitutive laws can be employed. This is indeed why these finite elements are called *general shell elements* (and sometimes also 'degenerated solid elements'); see the seminal work of Ahmad, Irons and Zienkiewicz (1970), and also Bathe (1996), Bischoff and Ramm (1997) and Başar and Krätzig (1989), and the references therein, for later generalizations of these concepts. This approach is widely used in practice, and evidence of its effectiveness can be found abundantly in the literature; see, for example, Bathe (1996). However, because of its specific construction, which does not rely on any shell theory, a mathematical analysis of such a procedure is very difficult to achieve.

The first objective of this article is to present some recent results that give a unified perspective of general shell elements in the framework of shell models and their discretizations. More specifically, we show that we can identify a well-defined shell model that 'underlies' general shell elements, that is, such that the finite element solutions converge to the exact solution of this model when the mesh is refined. In addition, we compare this model to other classical shell models by means of an asymptotic analysis. This unification of concepts paves the way for further mathematical analyses of these highly attractive numerical procedures.

A particularly important motivation for a thorough mathematical analysis of shell finite elements is the understanding and the treatment of some serious numerical pathologies that are known to occur when the thickness of the shell structure is 'small' (to fix the ideas, these phenomena typically become very significant as soon as the ratio of the thickness over the

https://doi.org/10.1017/S0962492901000034 Published online by Cambridge University Press

other characteristic dimensions of the structure is of the order of 1%, which is a situation commonly encountered in practice). The sources of these difficulties, including the by-now classical *numerical locking*, are now well identified, and they are closely related to the complexity and diversity of the asymptotic behaviour exhibited by shells; see Chapelle and Bathe (1998). However, from a numerical analysis perspective, a finite element procedure with proven reliability with respect to variation of the thickness parameter is still to be found. On the other hand, the literature abounds with allegedly reliable or locking-free shell finite elements, but the assessment performed to reach this conclusion is often inadequate or incomplete, when not altogether irrelevant. The second main objective of this article is thus to survey the issue of the reliability of shell finite elements with respect to variations of the thickness parameter. Of course, this issue must be put into perspective with the variations of behaviour induced in the exact solutions by variations of the thickness, namely with the analysis of the *asymptotic behaviour* of shell models.

This article is organized in the following manner. In Section 2 we present the two families of shell finite elements that we want to analyse and compare, namely the finite elements obtained by discretizing shell models (Section 2.1), and the general shell elements (Section 2.2). Section 3 is then dedicated to the issue of the reliability of shell finite elements. We start by surveying the asymptotic behaviour of shell models (Section 3.1) before focusing on computational issues (Section 3.2), and we conclude in Section 3.3 by presenting some guidelines for assessing and improving the reliability of shell finite elements.

In all our discussions we focus on linear formulations. Indeed, the difficulties that we want to analyse are already present in linear problems, hence it is natural to treat them in this framework first. Another simplification that we use is to assume that the thickness is constant (equal to 2ε) over the whole shell structure. This assumption is made only in order to simplify the formulas and the discussions, and does not represent a restriction in our analysis; see Bathe and Chapelle (200x) for a general analysis with arbitrary thickness.

Our notation is based on the notation used in the companion article (Ciarlet 2001) (see also Ciarlet (2000)); hence we do not repeat the same definitions here and we only define the new notation (mainly related to finite element concepts). In addition, we use the symbol C to denote a generic positive constant that, unless otherwise stated, is independent of all the parameters appearing in the same equation (and in particular of the mesh parameter h and of the thickness parameter ε), with the classical convention that C may take different values at each occurrence (even when appearing several times in the same equation).

https://doi.org/10.1017/S0962492901000034 Published online by Cambridge University Press

2. Two families of shell finite elements

2.1. Discretizations of classical shell models

As discussed in Ciarlet (2001), classical shell models are mathematical models in which the unknowns are defined on the mid-surface of the shell body or, equivalently, in the 2D reference domain ω from which the mid-surface is obtained via the mapping $\boldsymbol{\theta}$ (which we call the *chart*). In general, these models are based on kinematic assumptions that are used to describe the displacements of points located on material fibres that are orthogonal to the mid-surface in the original configuration. Roughly speaking, shell models can then be divided into two categories according to the kinematic assumption made.

(1) When the assumption is that any normal fibre remains straight and unstretched during the deformation, the displacements in the whole shell body are completely described by the data – on ω – of a displacement field and a rotation field. Namely, a displacement at any point in Ω^ε is given by

$$\boldsymbol{v}(x_1, x_2, x_3) = \boldsymbol{\eta}(x_1, x_2) + x_3 \boldsymbol{s}(x_1, x_2), \tag{2.1}$$

where $\boldsymbol{s}$, as the vector that represents the effect of the rotation of the normal fibre, is a vector tangent to the mid-surface at the point of coordinates (x_1, x_2), *i.e.*, $\boldsymbol{s} = s_\alpha \boldsymbol{a}^\alpha$. We call this the Reissner–Mindlin kinematic assumption, and the shell models that are based on this assumption the Reissner–Mindlin-type models; see Reissner (1945) and Mindlin (1951). As an example of this category of shell models, we will consider the model summarized in Naghdi (1963), which we call the Naghdi model.

(2) When the assumption is that any normal fibre remains straight, unstretched *and normal to the deformed mid-surface* (the so-called Kirchhoff–Love kinematic assumption), the displacements can be described by a displacement field only, that is,

$$\boldsymbol{v}(x_1, x_2, x_3) = \boldsymbol{\eta} - x_3(\eta_{3,\alpha} + b_\alpha^\sigma \eta_\sigma)\boldsymbol{a}^\alpha, \tag{2.2}$$

where $\boldsymbol{\eta}(x_1, x_2)$ is defined on ω. Note that, comparing (2.1) and (2.2), the additional assumption on the preserved orthogonality of fibres is equivalent to the rotation vector being given by

$$s_\alpha = -(\eta_{3,\alpha} + b_\alpha^\sigma \eta_\sigma). \tag{2.3}$$

We will call these shell models the Kirchhoff–Love-type models. The shell model proposed in Koiter (1966) belongs to this category and will henceforth be used as an example (we refer to this model as the Koiter model).

https://doi.org/10.1017/S0962492901000034 Published online by Cambridge University Press

An important difference between these two categories of models is the respective regularities of their solution spaces (which we also call the *displacement spaces*). Namely, for the Naghdi model the natural displacement space is

$$\boldsymbol{V}_N = \{(\boldsymbol{\eta}, \boldsymbol{s}) \in [H^1(\omega)]^5\} \cap \mathcal{BC}, \tag{2.4}$$

and

$$\boldsymbol{V}_K = \{\boldsymbol{\eta} \in [H^1(\omega)]^2 \times H^2(\omega)\} \cap \mathcal{BC} \tag{2.5}$$

for the Koiter model, where $\mathcal{BC}$ symbolically denotes the essential boundary conditions prescribed. Of course these boundary conditions must, in each case, be compatible with the nature of the functional space. Note that the discrepancy in the regularity of the transverse component of the displacement field (η_3) can be interpreted as the consequence of the additional constraint (2.3) acting on the solution space $\boldsymbol{V}_N$ where $\boldsymbol{s} \in [H^1(\omega)]^2$.

Clearly, in order to obtain well-posed variational formulations, some appropriate boundary conditions need to be prescribed in the displacement space. For the Naghdi and Koiter models (and indeed also for similar models from the above two categories), it can be shown that the corresponding bilinear forms are coercive and bounded on their respective displacement spaces provided that the boundary conditions are sufficient to prevent any rigid body motion of the shell body; see Bernadou and Ciarlet (1976) and Bernadou, Ciarlet and Miara (1994). Note that this holds in particular when the displacement field is set to zero on some part of the boundary $\partial\omega$ that does not correspond to a straight segment in the physical space. When the boundary conditions are compatible with the functional space considered and such that rigid body motions are prevented, we will say that we have *admissible boundary conditions*.

As a consequence, the discretization of classical shell models by conforming finite element methods is rather straightforward, at least in principle. The main difficulty lies in the required use of $\mathcal{C}^1$-conforming finite elements for the transverse displacements in models of Kirchhoff–Love type. These issues are thoroughly addressed in Bernadou (1996). Let us emphasize that these finite element procedures are based on meshes that are constructed in the *reference domain* ω, and on computations that require an extensive use of the chart $\boldsymbol{\theta}$. Since conforming methods are used, *a priori* error estimates follow from interpolation bounds and are of the type

$$\|\boldsymbol{\zeta} - \boldsymbol{\zeta}_h\|_{[H^1(\omega)]^3} + \|\boldsymbol{r} - \boldsymbol{r}_h\|_{[H^1(\omega)]^2} \leq Ch^p, \tag{2.6}$$

for the Naghdi model, and

$$\|\boldsymbol{\zeta} - \boldsymbol{\zeta}_h\|_{[H^1(\omega)]^2 \times H^2(\omega)} \leq Ch^p, \tag{2.7}$$

for the Koiter model, where the constants C and the orders of convergence p depend on the regularity of the exact solution and on the finite element

https://doi.org/10.1017/S0962492901000034 Published online by Cambridge University Press

shape functions considered. We emphasize that these estimates are not independent of the thickness parameter ε, as the constants C in (2.6)–(2.7) above depend on ε for two reasons:

- the coercivity and continuity constants of the corresponding bilinear forms depend on ε;
- the regularity bounds are not independent of ε in general.

This issue will be further addressed in Section 3.2.

In practice, in spite of the extensive use of shell finite elements in engineering, the type of finite element procedure that we have been describing in this section is not very often encountered.

2.2. General shell elements

Most shell finite element procedures used in engineering practice fall into this category of *general shell elements*. Unlike the previously discussed procedures, general shell elements are not derived from a shell model, but instead from a 3D variational formulation. A typical general shell element procedure is constructed as follows.

(1) Consider a general 3D variational formulation posed on the 3D geometrical domain defined by the mapping

$$\boldsymbol{\Theta}(x_1, x_2, x_3) = \boldsymbol{\theta}(x_1, x_2) + x_3 \boldsymbol{a}_3(x_1, x_2), \qquad (x_1, x_2, x_3) \in \omega \times]-\varepsilon, \varepsilon[, \tag{2.8}$$

and infer a modified variational problem from the *stress assumption*

$$\sigma^{33} \equiv 0. \tag{2.9}$$

We symbolically denote this modified problem by

$$B^{3D}(\boldsymbol{u}, \boldsymbol{v}) = L^{3D}(\boldsymbol{v}), \quad \forall \boldsymbol{v} \in \boldsymbol{V}^{3D}, \tag{2.10}$$

where B^{3D} and L^{3D} respectively represent the external and internal virtual works, and $\boldsymbol{V}^{3D}$ denotes the appropriate functional space, taking into account the essential boundary conditions.

(2) Consider a 2D mesh of ω given in the form of a set of points (the nodes) in ω and of a connectivity that defines the elements. Isoparametric elements are used; hence this defines a one-to-one mapping inside each element between the (x_1, x_2) coordinates and the local coordinates (ξ_1, ξ_2) of the form

$$\begin{pmatrix} x_1 \\ x_2 \end{pmatrix} = \sum_{i=1}^{k} \lambda_i(\xi_1, \xi_2) \begin{pmatrix} x_1^{(i)} \\ x_2^{(i)} \end{pmatrix}, \tag{2.11}$$

https://doi.org/10.1017/S0962492901000034 Published online by Cambridge University Press

where the functions λ_i are the shape functions associated with the k nodes of the element considered, and the quantities $(x_1^{(i)}, x_2^{(i)})$ denote the nodal coordinates. Of course, the shape functions depend on the polynomial order chosen and on the geometric type of the element (namely quadrilateral or triangular). Using this mapping, we define the interpolation operator $\mathcal{I}$ such that

$$\mathcal{I}(\phi)(x_1, x_2) = \sum_{i=1}^{k} \lambda_i(\xi_1, \xi_2)\, \phi(x_1^{(i)}, x_2^{(i)}) \tag{2.12}$$

in every element of the mesh, for any continuous scalar or vector function ϕ.

(3) Consider displacement functions defined over Ω^ε that satisfy *Reissner–Mindlin kinematic assumptions at all the nodes* of the mesh, and are interpolated inside the elements using the above shape functions, namely

$$\boldsymbol{v}(x_1, x_2, x_3) = \sum_{i=1}^{k} \lambda_i(\xi_1, \xi_2)(\boldsymbol{\eta}^{(i)} + x_3 \boldsymbol{s}^{(i)}), \tag{2.13}$$

where $\boldsymbol{s}^{(i)}$ corresponds to a rotation at node i, and hence satisfies

$$\boldsymbol{s}^{(i)} \cdot \boldsymbol{a}_3^{(i)} = 0. \tag{2.14}$$

We call $\boldsymbol{V}_h^{3D}$ the space of functions of this type that satisfy the boundary conditions prescribed on the structure (note that boundary conditions can be prescribed here as they would be for a Reissner–Mindlin-type model).

(4) Consider the problem:
Find $\boldsymbol{u} \in \boldsymbol{V}_h^{3D}$ such that

$$B_h^{3D}(\boldsymbol{u}, \boldsymbol{v}) = L_h^{3D}(\boldsymbol{v}), \quad \forall \boldsymbol{v} \in \boldsymbol{V}_h^{3D}, \tag{2.15}$$

where B_h^{3D} and L_h^{3D} are obtained from B^{3D} and L^{3D} by using, instead of the exact chart $\boldsymbol{\Theta}$, the approximation

$$\boldsymbol{\Theta}_h(x_1, x_2, x_3) = \mathcal{I}(\boldsymbol{\theta})(x_1, x_2) + x_3 \mathcal{I}(\boldsymbol{a}_3)(x_1, x_2), \tag{2.16}$$

to be compared with (2.8).

The general shell element procedure consists in solving problem (2.15), hence the unknowns (degrees of freedom) are the 3 displacement components and the 2 rotation components at the nodes. Note that the degrees of freedom are similar to those of a classical shell finite element procedure obtained by discretizing a Reissner–Mindlin-type model. However, it appears from the above description that general shell elements have two key advantages.

https://doi.org/10.1017/S0962492901000034 Published online by Cambridge University Press

- They are not obtained from a specific shell model, but from a *general* 3D formulation, hence they can be easily used for arbitrary 3D material laws and also for nonlinear formulations. This is indeed why these procedures are called *general* shell elements.
- As implied by the use of the approximate chart $\boldsymbol{\Theta}_h$, the derivation of the associated matrix problem does not require the data of the exact mid-surface chart $\boldsymbol{\theta}$, but only the position of the points and the value of the normal vectors at the nodes. This is extremely convenient in practice as most structures analysed are the result of design procedures (CAD systems) that do not provide these charts.

The connections between general shell elements and classical shell elements (*i.e.*, those obtained by discretizing classical shell models) have remained unclear for many years. Moreover, this issue has probably been a source of major misunderstanding between the engineering community (primarily using and developing general shell elements) and the numerical analysis community (considering only classical shell elements). These connections are now much better identified; see in particular Chapelle and Bathe (2000). Indeed, for a given 3D material law we can consider the problem:
Find $(\boldsymbol{\zeta}, \boldsymbol{r})$ in $\boldsymbol{V}_N$ such that

$$B^{3D}(\boldsymbol{\zeta} + x_3\boldsymbol{r}, \boldsymbol{\eta} + x_3\boldsymbol{s}) = L^{3D}(\boldsymbol{\eta} + x_3\boldsymbol{s}), \quad \forall(\boldsymbol{\eta}, \boldsymbol{s}) \in \boldsymbol{V}_N. \tag{2.17}$$

Clearly, this defines a shell model of Reissner–Mindlin type, since the unknowns are a displacement field and a rotation field, both being given on the mid-surface (or in the reference domain). This shell model is the natural candidate for being the model that underlies general shell elements, *i.e.*, the model that provides the solution to which finite element solutions converge when the mesh parameter h (namely the diameter of the largest element) tends to zero. With a view to analysing problem (2.15) as an internal approximation of problem (2.17), we define V_h as the scalar finite element space associated with the isoparametric discretization above, *i.e.*, a function ϕ is in V_h if and only if $\phi = \mathcal{I}(\phi)$. Note that $V_h \subset H^1(\omega)$. Then $\boldsymbol{v} \in \boldsymbol{V}_h^{3D}$ is equivalent to

$$\boldsymbol{v} = \boldsymbol{\eta}(x_1, x_2) + x_3\,\tilde{\boldsymbol{s}}(x_1, x_2), \tag{2.18}$$

with the three conditions:

C1 $\boldsymbol{\eta} \cdot \hat{\boldsymbol{e}}_i \in V_h$ and $\tilde{\boldsymbol{s}} \cdot \hat{\boldsymbol{e}}_i \in V_h$ for $i = 1, 2, 3$;
C2 $\tilde{\boldsymbol{s}} \cdot \boldsymbol{a}_3 = 0$ at all the nodes of the mesh;
C3 $\boldsymbol{\eta}$ and $\tilde{\boldsymbol{s}}$ satisfy the proper boundary conditions.

Denoting by π the operator that projects a vector field defined over ω onto the tangential plane of the mid-surface at each point, that is,

$$\pi(\tilde{\boldsymbol{s}}) = \tilde{\boldsymbol{s}} - (\tilde{\boldsymbol{s}} \cdot \boldsymbol{a}_3)\boldsymbol{a}_3, \tag{2.19}$$

https://doi.org/10.1017/S0962492901000034 Published online by Cambridge University Press

we define the finite element space $\boldsymbol{V}_{Nh}$ as the set of functions $(\boldsymbol{\eta}, \pi(\tilde{\boldsymbol{s}}))$ such that $(\boldsymbol{\eta}, \tilde{\boldsymbol{s}})$ satisfies the three conditions (C1, C2, C3) above. Clearly $\boldsymbol{V}_{Nh}$ is a (finite-dimensional) subspace of $\boldsymbol{V}_N$. Note that the use of the projection operator is required for that purpose because we do not directly have $\tilde{\boldsymbol{s}}$ in the tangential plane at every point of ω. Using the equivalence

$$\pi(\tilde{\boldsymbol{s}}) = \boldsymbol{s} \Leftrightarrow \tilde{\boldsymbol{s}} = \mathcal{I}(\boldsymbol{s}), \tag{2.20}$$

valid for any $(\boldsymbol{\eta}, \pi(\tilde{\boldsymbol{s}}))$ in $\boldsymbol{V}_{Nh}$, we can then reformulate the general shell element procedure as follows:
Find $(\boldsymbol{\zeta}, \boldsymbol{r})$ in $\boldsymbol{V}_{Nh}$ such that

$$B_h^{3D}(\boldsymbol{\zeta} + x_3\,\mathcal{I}(\boldsymbol{r}), \boldsymbol{\eta} + x_3\,\mathcal{I}(\boldsymbol{s})) = L_h^{3D}(\boldsymbol{\eta} + x_3\,\mathcal{I}(\boldsymbol{s})),\ \forall (\boldsymbol{\eta}, \boldsymbol{s}) \in \boldsymbol{V}_{Nh}. \tag{2.21}$$

Now comparing this equation with the continuous problem (2.17), we can say that the general shell element procedure corresponds to a discretization scheme of the continuous problem with approximate bilinear and linear forms (see, *e.g.*, Ciarlet (1978)), and we observe that consistency errors come from two sources: the approximation of the geometry corresponding to equation (2.16) and the presence of the interpolation operator in (2.21).

When choosing specific 3D formulations, the connection between the shell model represented by (2.17) and the corresponding general shell element procedure can be further analysed. In particular, when considering Hooke's constitutive law we obtain, as shown in Chapelle and Bathe (2000),

$$\begin{aligned} B^{3D}(\boldsymbol{u}, \boldsymbol{v}) = \int_{\Omega^\varepsilon} [\tfrac{1}{2} g^{\alpha\beta\sigma\tau} e_{\alpha||\beta}(\boldsymbol{u}) e_{\sigma||\tau}(\boldsymbol{v}) \\ + 4\mu g^{\alpha\beta} e_{\alpha||3}(\boldsymbol{u}) e_{\beta||3}(\boldsymbol{v})] \sqrt{g}\ \mathrm{d}x, \end{aligned} \tag{2.22}$$

with

$$g^{\alpha\beta\sigma\tau} = \tfrac{4\lambda\mu}{\lambda+2\mu} g^{\alpha\beta} g^{\sigma\tau} + 2\mu(g^{\alpha\sigma} g^{\beta\tau} + g^{\alpha\tau} g^{\beta\sigma}). \tag{2.23}$$

Note that we assume that the Lamé constants do not depend on ε. Taking into account the Reissner–Mindlin kinematic assumption, we have

$$\begin{cases} e_{\sigma||\tau}(\boldsymbol{\eta} + x_3\boldsymbol{s}) = \gamma_{\sigma\tau}(\boldsymbol{\eta}) - x_3\,\rho^N_{\sigma\tau}(\boldsymbol{\eta}, \boldsymbol{s}) - (x_3)^2 \kappa_{\sigma\tau}(\boldsymbol{s}), \\ e_{\beta||3}(\boldsymbol{\eta} + x_3\boldsymbol{s}) = \gamma_{\beta 3}(\boldsymbol{\eta}, \boldsymbol{s}), \end{cases} \tag{2.24}$$

where we recall that $\gamma_{\sigma\tau}$, $\rho^N_{\sigma\tau}$ and $\gamma_{\beta 3}$ respectively represent the components of the tensors of membrane strains, bending (or flexural) strains and shear strains in the Naghdi model, and $\kappa_{\sigma\tau}$ corresponds to a new tensor defined by

$$\kappa_{\sigma\tau}(\boldsymbol{s}) = \tfrac{1}{2}(b^\alpha_\sigma s_{\alpha|\tau} + b^\alpha_\tau s_{\alpha|\sigma}). \tag{2.25}$$

In addition, we consider the external virtual work given by

$$L^{3D}(\boldsymbol{v}) = \int_{\Omega^\varepsilon} \boldsymbol{f} \cdot \boldsymbol{v}\, \sqrt{g}\ \mathrm{d}x, \tag{2.26}$$

https://doi.org/10.1017/S0962492901000034 Published online by Cambridge University Press

i.e., $\boldsymbol{f}$ represents the applied distributed force, and we assume $\boldsymbol{f} \in [L^2(\Omega^\varepsilon)]^3$. We then have the following result, under standard assumptions regarding the mesh and the finite element shape functions used; see Chapelle and Bathe (2000).

Proposition 1. Provided that the boundary conditions are admissible, problem (2.17) has a unique solution. Moreover, this solution is the limit of the solutions of Problem (2.15) when the mesh parameter h tends to zero.

This result shows that (at least in the case of Hooke's law) the shell model given by (2.17) really is the mathematical model that underlies general shell element procedures. It is then important to investigate the relations between this shell model (which we call the *basic shell model*; see Bathe and Chapelle (200x)) and classical shell models. If we formally transform the expression (2.22) by truncating the expansions in powers of x_3 of the expressions appearing under the integral sign, taking

- the first-order approximation of the strains, namely

$$\begin{cases} e_{\sigma||\tau}(\boldsymbol{\eta} + x_3\boldsymbol{s}) \approx \gamma_{\sigma\tau}(\boldsymbol{\eta}) - x_3\,\rho^N_{\sigma\tau}(\boldsymbol{\eta}, \boldsymbol{s}), \\ e_{\beta||3}(\boldsymbol{\eta} + x_3\boldsymbol{s}) = \gamma_{\beta 3}(\boldsymbol{\eta}, \boldsymbol{s}), \end{cases} \tag{2.27}$$

- the zero-order approximation of all geometric coefficients, namely

$$g^{\alpha\beta\sigma\tau} \approx a^{\alpha\beta\sigma\tau}, \quad g^{\alpha\beta} \approx a^{\alpha\beta}, \quad \sqrt{g} \approx \sqrt{a}, \tag{2.28}$$

we obtain exactly the bilinear form of the Naghdi model (with $c = 8$ in the equations recalled in Ciarlet (2001)); see Chapelle and Bathe (2000), and also Delfour (1998) where various combinations of truncations are considered and analysed. This suggests that some close connections exist between the basic model and the Naghdi model. We will further substantiate these connections in Section 3.1 by showing that the two models are *asymptotically equivalent* as regards their asymptotic solutions when the thickness parameter tends to zero.

As a conclusion, we can say that, although they do not seem (at first sight) to bear much resemblance to classical shell elements, general shell elements are – in fact – non-conforming discretization schemes of a shell model of Reissner–Mindlin type which is itself very closely connected to the Naghdi model. This is extremely important, as it allows us to analyse finite element procedures of both 'families' using similar tools. As a matter of fact, further advances in the analysis of some specific general shell procedures have already been obtained with this approach (*cf.*, *e.g.*, Malinen (2000)), in particular as regards the reliability of shell finite elements, which is the subject of our next section.

https://doi.org/10.1017/S0962492901000034 Published online by Cambridge University Press

3. Computational reliability issues for thin shells

The essential motivation underlying the formulation of shell models and shell finite elements is the reduction of the cost of the analysis (in particular the computational cost), compared to the cost of a full 3D analysis, by instead considering a 2D problem. This motivation is based on the assumption (or the 'hope') that the accuracy of the solution obtained only depends on criteria that prevail in *2D* analysis, that is, typically on the fineness of the 2D mesh *regardless of the third dimension*, namely the thickness of the structure. This means that we implicitly expect uniform convergence of the finite element solution with respect to the thickness parameter, namely, error bounds of the type

$$\frac{\|\boldsymbol{\zeta}^\varepsilon - \boldsymbol{\zeta}_h^\varepsilon\|_*}{\|\boldsymbol{\zeta}^\varepsilon\|_*} \leq Ch^p, \tag{3.1}$$

where we now use ε as a superscript to indicate that the solutions depend on this parameter, and where C (and also p) *should not depend on* ε. We subscript the norm symbol with a '$*$' to signify that we do not necessarily require that uniform convergence hold in the Sobolev space in which the problem is originally set (for example $[H^1(\omega)]^2 \times H^2(\omega)$ for Kirchhoff–Love-type models), but that we may tolerate uniform convergence in weaker norms to be defined.

Unfortunately, it was soon recognized that standard finite element methods (such as the ones that we described in the previous section) do not provide such uniform bounds in general. The reason for this will be analysed in Section 3.2. To that purpose it is necessary to start by surveying the behaviour of the exact solution of the shell model when the thickness parameter tends to zero, namely the asymptotic behaviour of shell models, which is the objective of the forthcoming section. This analysis will, in particular, allow us to specify the norms in which we seek uniform estimates for approximate solutions.

3.1. Asymptotic behaviour of shell models

Most classical shell models can be written in the following generic form: Find $\boldsymbol{Z}^\varepsilon \in \boldsymbol{V}$ such that

$$\varepsilon^3 B_F(\boldsymbol{Z}^\varepsilon, \boldsymbol{E}) + \varepsilon B_M(\boldsymbol{Z}^\varepsilon, \boldsymbol{E}) = L^\varepsilon(\boldsymbol{E}), \quad \forall \boldsymbol{E} \in \boldsymbol{V}. \tag{3.2}$$

The meaning of the symbols appearing in this formulation is as follows.

- $\boldsymbol{Z}^\varepsilon$: the unknown solution, namely the displacement of the mid-surface for a Kirchhoff–Love-type model, or this displacement *and* the rotation of the normal fibre for a Reissner–Mindlin-type model.
- $\boldsymbol{E}$: a corresponding test function that we call a 'displacement' (even though it also contains a rotation for a Reissner–Mindlin-type model).

https://doi.org/10.1017/S0962492901000034 Published online by Cambridge University Press

- $\boldsymbol{V}$: the solution space (we recall that the definition of this space takes into account the essential boundary conditions).
- B_F: a scaled representation of the bending (flexural) energy.
- B_M: a scaled representation of the membrane energy for a Kirchhoff–Love-type model, or of the membrane energy *and* the shear energy for a Reissner–Mindlin-type model.
- $L^\varepsilon(\boldsymbol{E})$: the external virtual work associated with $\boldsymbol{E}$.

For example, for the Koiter model we have, as seen in Koiter (1966),

$$B_F^K(\boldsymbol{\zeta},\boldsymbol{\eta}) = \tfrac{1}{3}\int_\omega a^{\alpha\beta\sigma\tau}\rho_{\alpha\beta}(\boldsymbol{\zeta})\rho_{\sigma\tau}(\boldsymbol{\eta})\sqrt{a}\,\mathrm{d}y, \tag{3.3}$$

$$B_M^K(\boldsymbol{\zeta},\boldsymbol{\eta}) = \int_\omega a^{\alpha\beta\sigma\tau}\gamma_{\alpha\beta}(\boldsymbol{\zeta})\gamma_{\sigma\tau}(\boldsymbol{\eta})\sqrt{a}\,\mathrm{d}y, \tag{3.4}$$

and for the Naghdi model

$$B_F^N((\boldsymbol{\zeta},\boldsymbol{r}),(\boldsymbol{\eta},\boldsymbol{s})) = \tfrac{1}{3}\int_\omega a^{\alpha\beta\sigma\tau}\rho^N_{\alpha\beta}(\boldsymbol{\zeta},\boldsymbol{r})\rho^N_{\sigma\tau}(\boldsymbol{\eta},\boldsymbol{s})\sqrt{a}\,\mathrm{d}y, \tag{3.5}$$

$$B_M^N((\boldsymbol{\zeta},\boldsymbol{r}),(\boldsymbol{\eta},\boldsymbol{s})) = \int_\omega [a^{\alpha\beta\sigma\tau}\gamma_{\alpha\beta}(\boldsymbol{\zeta})\gamma_{\sigma\tau}(\boldsymbol{\eta}) + c\mu a^{\alpha\beta}\gamma_{\alpha3}(\boldsymbol{\zeta},\boldsymbol{r})\gamma_{\beta3}(\boldsymbol{\eta},\boldsymbol{s})]\sqrt{a}\,\mathrm{d}y. \tag{3.6}$$

We further emphasize that, in (3.2), *the expressions of the bilinear forms B_F and B_M do not depend on the thickness parameter ε*. We also introduced ε as a superscript in the right-hand side of the formulation because it is unlikely to obtain well-posed asymptotic behaviour while keeping the loading constant over the whole sequence of problems. More specifically, what we will be looking for in the asymptotic analysis is a scaling of the right-hand side in the form

$$L^\varepsilon(\boldsymbol{E}) = \varepsilon^\rho G(\boldsymbol{E}), \tag{3.7}$$

where G is a function of $\boldsymbol{V}'$ *independent of* ε and ρ is a real number, for which the scaled external work $G(\boldsymbol{Z}^\varepsilon)$ converges to a *finite and nonzero* limit when ε tends to zero. In this case, we will say that the given scaling provides *admissible asymptotic behaviour*. Of course, this is equivalent to requiring that the scaled internal work $\varepsilon^{3-\rho}B_F(\boldsymbol{Z}^\varepsilon,\boldsymbol{Z}^\varepsilon) + \varepsilon^{1-\rho}B_M(\boldsymbol{Z}^\varepsilon,\boldsymbol{Z}^\varepsilon)$ have a finite nonzero limit, since

$$\varepsilon^{3-\rho}B_F(\boldsymbol{Z}^\varepsilon,\boldsymbol{Z}^\varepsilon) + \varepsilon^{1-\rho}B_M(\boldsymbol{Z}^\varepsilon,\boldsymbol{Z}^\varepsilon) = G(\boldsymbol{Z}^\varepsilon). \tag{3.8}$$

We can then show the following result; see Blouza, Brezzi and Lovadina (1999), Baiocchi and Lovadina (200x) and Bathe and Chapelle (200x).

https://doi.org/10.1017/S0962492901000034 Published online by Cambridge University Press

Proposition 2. There is at most one exponent ρ that provides admissible asymptotic behaviour. In addition, if such a number exists we have

$$1 \leq \rho \leq 3. \tag{3.9}$$

Remark. In some cases the convergence may also be such that the sequence $(\boldsymbol{Z}^\varepsilon)$ tends to some limit in $\boldsymbol{V}$, but we want to allow for more general situations in which a weaker convergence property may hold.

As discussed in Sanchez-Hubert and Sanchez-Palencia (1997) (see also Ciarlet (2001) for the Koiter model), classical shell models feature asymptotic behaviour that dramatically differs according to the contents of the subspace:

$$\boldsymbol{V}_F = \{\boldsymbol{E} \in \boldsymbol{V} : B_M(\boldsymbol{E}, \boldsymbol{E}) = 0\}. \tag{3.10}$$

This subspace contains the displacements that have zero membrane energy (and also zero shear energy for Reissner–Mindlin-type models). For this reason, these displacements are called *pure-bending displacements* (since only the bending energy is nonzero). As a matter of fact, because of the severe kinematic constraints corresponding to zero membrane strains (3 equations versus 3 components of displacements), it may very well happen that

$$\boldsymbol{V}_F = \{\boldsymbol{0}\}. \tag{3.11}$$

In this case we say that *pure bending is inhibited*. This situation induces asymptotic behaviour very different from when pure bending is not inhibited. The existence of nonzero pure bending displacements is governed by the geometry of the mid-surface and the boundary conditions prescribed on the structure (we further analyse this issue below).

We start by considering the case of non-inhibited pure bending. It can then be shown that well-defined asymptotic behaviour exists for $\rho = 3$. In this case, the variational formulation can indeed be re-written as

$$B_F(\boldsymbol{Z}^\varepsilon, \boldsymbol{E}) + \frac{1}{\varepsilon^2} B_M(\boldsymbol{Z}^\varepsilon, \boldsymbol{E}) = G(\boldsymbol{E}), \quad \forall \boldsymbol{E} \in \boldsymbol{V}. \tag{3.12}$$

Since ε is a small parameter, this equation can be interpreted as the *penalized form* of a problem in which the solution $\boldsymbol{Z}^0$ is constrained to lie in the subspace $\boldsymbol{V}_F$. Namely, the candidate limit problem for (3.12) is:
Find $\boldsymbol{Z}^0$ in $\boldsymbol{V}_F$ such that

$$B_F(\boldsymbol{Z}^0, \boldsymbol{E}) = G(\boldsymbol{E}), \quad \forall \boldsymbol{E} \in \boldsymbol{V}_F. \tag{3.13}$$

Note that this problem is well-posed, since it corresponds to the restriction to $\boldsymbol{V}_F$, a closed subspace of $\boldsymbol{V}$, of the minimization problem equivalent to the original variational formulation. We then have the following result; see Chenais and Paumier (1994), and also Pitkäranta (1992) and Sanchez-Palencia (1992).

https://doi.org/10.1017/S0962492901000034 Published online by Cambridge University Press

Proposition 3. Assume that pure bending is not inhibited. Then, setting $\rho = 3$, $\boldsymbol{Z}^\varepsilon$ converges strongly in $\boldsymbol{V}$ to $\boldsymbol{Z}^0$, the solution of (3.13). In addition we have

$$\lim_{\varepsilon \to 0} \frac{1}{\varepsilon^2} B_M(\boldsymbol{Z}^\varepsilon, \boldsymbol{Z}^\varepsilon) = 0. \tag{3.14}$$

Equation (3.14) shows that, in the scaled deformation energy, the part corresponding to the membrane energy (and also the part corresponding to the shear energy when applicable) tends to zero, while the part that corresponds to bending deformations tends to a finite value. This is why this asymptotic behaviour is also called *bending-dominated behaviour*.

Note that, when pure bending is not inhibited, Proposition 3 shows that we have admissible asymptotic behaviour for the scaling $\rho = 3$ *provided that* $\boldsymbol{Z}^0$ *is nonzero*. If $\boldsymbol{Z}^0 = \boldsymbol{0}$, that is, if and only if

$$G(\boldsymbol{E}) = 0, \quad \forall \boldsymbol{E} \in \boldsymbol{V}_F, \tag{3.15}$$

another admissible scaling (for $1 \leq \rho < 3$) may exist. This, however, does not correspond to a 'physical situation' as small perturbations in the geometry (producing variations in $\boldsymbol{V}_F$) or in the loading lead to a violation of (3.15), hence to effects of smaller asymptotic order, namely of 'larger magnitude' (corresponding to bending-dominated behaviour, that is, $\rho = 3$). Therefore we do not further consider this situation; see Chapelle and Bathe (1998) for a more detailed analysis of this issue.

By contrast, when pure bending is inhibited (which is a situation more common than the previous one, although both may be encountered in practice – see Ciarlet (2001) and Bathe and Chapelle (200x)), the asymptotic behaviour is very different and more complex. We consider the tentative scaling $\rho = 1$. The variational formulation then gives

$$B_M(\boldsymbol{Z}^\varepsilon, \boldsymbol{E}) + \varepsilon^2 B_F(\boldsymbol{Z}^\varepsilon, \boldsymbol{E}) = G(\boldsymbol{E}), \quad \forall \boldsymbol{E} \in \boldsymbol{V}, \tag{3.16}$$

and we note that

$$\|\boldsymbol{E}\|_M = [B_M(\boldsymbol{E}, \boldsymbol{E})]^{\frac{1}{2}} \tag{3.17}$$

defines a norm over $\boldsymbol{V}$ which, of course, satisfies

$$\|\boldsymbol{E}\|_M \leq C \|\boldsymbol{E}\|_{\boldsymbol{V}}, \quad \forall \boldsymbol{E} \in \boldsymbol{V}, \tag{3.18}$$

but is not equivalent to the original norm (*cf.* examples of the Koiter and Naghdi models above). We call this new norm the *membrane energy norm*. We then recognize in (3.16) a *singular perturbation problem*. Defining $\boldsymbol{V}_M$ as the space obtained by completion of $\boldsymbol{V}$ for the membrane energy norm, we introduce the variational problem:
Find $\boldsymbol{Z}^M$ in $\boldsymbol{V}_M$ such that

$$B_M(\boldsymbol{Z}^M, \boldsymbol{E}) = G(\boldsymbol{E}), \quad \forall \boldsymbol{E} \in \boldsymbol{V}_M. \tag{3.19}$$

https://doi.org/10.1017/S0962492901000034 Published online by Cambridge University Press

Clearly, this problem is well-posed *provided that* $G \in (\boldsymbol{V}_M)'$. Note that this corresponds to a restriction on the loading since $(\boldsymbol{V}_M)' \subset \boldsymbol{V}'$. An equivalent way of writing this condition is

$$|G(\boldsymbol{E})| \leq C[B_M(\boldsymbol{E}, \boldsymbol{E})]^{\frac{1}{2}}, \quad \forall \boldsymbol{E} \in \boldsymbol{V} \tag{3.20}$$

since, by density considerations, this is equivalent to the same condition holding for any $\boldsymbol{E} \in \boldsymbol{V}_M$. Under this assumption we have admissible asymptotic behaviour as shown in the following proposition; see Lions (1973).

Proposition 4. Assume that pure bending is inhibited and that $G \in (\boldsymbol{V}_M)'$. Then, setting $\rho = 1$, $\boldsymbol{Z}^\varepsilon$ converges strongly in $\boldsymbol{V}_M$ to $\boldsymbol{Z}^M$, the solution of (3.19). In addition we have

$$\lim_{\varepsilon \to 0} \varepsilon^2 B_F(\boldsymbol{Z}^\varepsilon, \boldsymbol{Z}^\varepsilon) = 0. \tag{3.21}$$

Since, by (3.21), the bending part of the scaled energy tends to zero while the remaining part (the membrane part, and also the shear part for Reissner–Mindlin-type models) tends to a finite value, this asymptotic behaviour is called *membrane-dominated behaviour*. Note that (under the assumptions of the proposition) we always have admissible asymptotic behaviour since $\boldsymbol{Z}^M$ cannot be zero (unless, of course, G is zero).

We have therefore identified two very distinct categories of admissible asymptotic behaviour for classical shell models: bending-dominated behaviour and membrane-dominated behaviour. It is the contents of the subspace $\boldsymbol{V}_F$ that determine into which category a given problem falls. For each of these types of asymptotic behaviour, convergence of the solutions is obtained in a given norm, hence it is natural to seek uniform convergence of finite element solutions in the same norm (*cf.* the next section). Other types of asymptotic behaviour may exist and the above discussion shows that they can arise only when pure bending is inhibited and $G \notin (\boldsymbol{V}_M)'$ (disregarding cases when (3.15) holds, for the above-mentioned reason). These situations are more complex than the two 'clear-cut' asymptotic behaviour types discussed, and they have not yet been completely elucidated, although significant advances have been made in their analysis; see in particular Pitkäranta and Sanchez-Palencia (1997) (*cf.* also Section 3.3).

We now consider the case of the basic shell model, namely the shell model that underlies general shell element. We recall that the general asymptotic analysis performed above is not directly applicable to this model since it cannot be written in the form (3.2). In particular the membrane and bending deformation energies are coupled in the term

$$\int_{\Omega^\varepsilon} \tfrac{1}{2} g^{\alpha\beta\sigma\tau} e_{\alpha||\beta}(\boldsymbol{u}) e_{\sigma||\tau}(\boldsymbol{v}) \sqrt{g}\, \mathrm{d}x, \tag{3.22}$$

https://doi.org/10.1017/S0962492901000034 Published online by Cambridge University Press

as shown in (2.24). Another significant difference is that the loading acting on the structure is three-dimensional, taking the form

$$L^{(3D)}(\boldsymbol{v}) = \int_{\Omega^\varepsilon} \boldsymbol{f}^\varepsilon \cdot \boldsymbol{v}\, \sqrt{g}\, \mathrm{d}x. \tag{3.23}$$

In order to perform an asymptotic analysis consistent with the general one above, we consider the asymptotic assumption

$$\boldsymbol{f}^\varepsilon = \varepsilon^{\rho-1}\boldsymbol{g}, \tag{3.24}$$

recalling that the external work involves an integration over the thickness. Furthermore, we assume that $\boldsymbol{g}$ is sufficiently regular to allow the following expansion:

$$\boldsymbol{g}(x_1, x_2, x_3) = \boldsymbol{g}_0(x_1, x_2) + x_3\boldsymbol{g}_1(x_1, x_2) + (x_3)^2\boldsymbol{g}_2(x_1, x_2, x_3), \tag{3.25}$$

where $\boldsymbol{g}_0$ and $\boldsymbol{g}_1$ are in $L^2(\omega)$, while $\boldsymbol{g}_2$ is a bounded function. Let $(\boldsymbol{\zeta}^\varepsilon, \boldsymbol{r}^\varepsilon)$ be the solution of the basic shell model, that is:
Find $(\boldsymbol{\zeta}^\varepsilon, \boldsymbol{r}^\varepsilon) \in \boldsymbol{V}_N$ such that

$$B^{3D}(\boldsymbol{\zeta}^\varepsilon + x_3\boldsymbol{r}^\varepsilon, \boldsymbol{\eta} + x_3\boldsymbol{s}) = \varepsilon^{\rho-1}\int_{\Omega^\varepsilon} \boldsymbol{g}\cdot(\boldsymbol{\eta} + x_3\boldsymbol{s})\sqrt{g}\, \mathrm{d}x, \quad \forall(\boldsymbol{\eta}, \boldsymbol{s}) \in \boldsymbol{V}_N. \tag{3.26}$$

We also introduce the following Naghdi problem:
Find $(\tilde{\boldsymbol{\zeta}}^\varepsilon, \tilde{\boldsymbol{r}}^\varepsilon) \in \boldsymbol{V}_N$ such that

$$\varepsilon^3 B_F^N((\tilde{\boldsymbol{\zeta}}^\varepsilon, \tilde{\boldsymbol{r}}^\varepsilon), (\boldsymbol{\eta}, \boldsymbol{s})) + \varepsilon B_M^N((\tilde{\boldsymbol{\zeta}}^\varepsilon, \tilde{\boldsymbol{r}}^\varepsilon), (\boldsymbol{\eta}, \boldsymbol{s})) = \varepsilon^{\rho-1}G(\boldsymbol{\eta}), \quad \forall(\boldsymbol{\eta}, \boldsymbol{s}) \in \boldsymbol{V}_N, \tag{3.27}$$

where

$$G(\boldsymbol{\eta}) = \int_\omega \boldsymbol{g}_0 \cdot \boldsymbol{\eta}\sqrt{a}\, \mathrm{d}y, \tag{3.28}$$

and setting $c = 8$ in B_F^N; see Ciarlet (2001). Calling $\boldsymbol{V}_F^N$ the pure-bending displacement subspace relative to this Naghdi problem (3.27), and $\boldsymbol{V}_M^N$ the completed space for the membrane energy norm when pure bending is inhibited, we then have the following asymptotic properties (assuming the chart is smooth); see Chapelle and Bathe (2000).

Proposition 5. If pure bending is not inhibited in the Naghdi problem (3.27), then for the scaling $\rho = 3$ both sequences $(\boldsymbol{\zeta}^\varepsilon, \boldsymbol{r}^\varepsilon)$ and $(\tilde{\boldsymbol{\zeta}}^\varepsilon, \tilde{\boldsymbol{r}}^\varepsilon)$ converge in $\boldsymbol{V}_N$ to the same limit $(\boldsymbol{\zeta}^0, \boldsymbol{r}^0)$, which is the element of $\boldsymbol{V}_F^N$ that satisfies

$$B_F^N((\boldsymbol{\zeta}^0, \boldsymbol{r}^0), (\boldsymbol{\eta}, \boldsymbol{s})) = G(\boldsymbol{\eta}), \quad \forall(\boldsymbol{\eta}, \boldsymbol{s}) \in \boldsymbol{V}_F^N. \tag{3.29}$$

Alternatively, if pure bending is inhibited and if $G \in (\boldsymbol{V}_F^N)'$, then for the

https://doi.org/10.1017/S0962492901000034 Published online by Cambridge University Press

scaling $\rho = 1$ both sequences $(\boldsymbol{\zeta}^\varepsilon, \boldsymbol{r}^\varepsilon)$ and $(\tilde{\boldsymbol{\zeta}}^\varepsilon, \tilde{\boldsymbol{r}}^\varepsilon)$ converge in $\boldsymbol{V}_M^N$ to the same limit $(\boldsymbol{\zeta}^M, \boldsymbol{r}^M)$, which is the element of $\boldsymbol{V}_M^N$ that satisfies

$$B_M^N((\boldsymbol{\zeta}^M, \boldsymbol{r}^M), (\boldsymbol{\eta}, \boldsymbol{s})) = G(\boldsymbol{\eta}) \quad \forall (\boldsymbol{\eta}, \boldsymbol{s}) \in \boldsymbol{V}_M^N. \tag{3.30}$$

Therefore, the solution of the basic shell model converges to the same limit solutions and under the exact same assumptions as the solution of the Naghdi problem (3.27). To summarize these properties, we will say that the basic shell model and the Naghdi model are 'asymptotically equivalent'.

We close this section by providing some guidelines for the analysis of the subspace of pure bending displacements, since the contents of this subspace have been shown to crucially determine the asymptotic behaviour of the shell problems. First of all we note that, for both Kirchhoff–Love-type and Reissner–Mindlin-type models, pure bending displacements have identically zero membrane strains. In addition, for a Reissner–Mindlin-type model pure bending displacements also have zero shear strains. However, the condition of zero shear strains can be written in the form of an explicit expression giving the rotation field $\boldsymbol{\eta}$ in terms of the displacement field $\boldsymbol{s}$, namely

$$\eta_\alpha = -(s_{3,\alpha} + b_\alpha^\sigma s_\sigma). \tag{3.31}$$

By contrast, the condition of vanishing membrane strains

$$\gamma_{\alpha\beta}(\boldsymbol{\eta}) = 0, \quad \forall \alpha, \beta = 1, 2, \tag{3.32}$$

make up an exactly determined differential system (three equations versus three unknowns) that must be satisfied by the displacement field only. Hence this is clearly the crucial condition that determines the contents of the pure bending displacement subspace, which is why elements of this subspace are also called *inextensional displacements* (we recall that the membrane strain tensor is the tensor of linearized change of metric of the mid-surface – see Koiter (1966)), even in the case of Reissner–Mindlin-type models. In addition, system (3.32) enjoys the following remarkable property (*cf.* Sanchez-Palencia (1989*a*, 1989*b*) and the references therein).

Proposition 6. The differential nature (elliptic, parabolic or hyperbolic) of system (3.32) is the same as the geometric nature of the mid-surface at the point in consideration. Furthermore, when such a concept is relevant (namely in the hyperbolic and – by extension – parabolic case) the characteristics of the system are also the asymptotic lines of the surface.

This property is extremely valuable for analysing the contents of the subspace of pure bending displacements. In particular it shows how the geometry (*i.e.*, the type of mid-surface) and the boundary conditions can affect the contents of the subspace (*cf.*, *e.g.*, Chapelle and Bathe (1998) for examples). We refer to Sanchez-Hubert and Sanchez-Palencia (1997) for a more detailed analysis of this issue.

https://doi.org/10.1017/S0962492901000034 Published online by Cambridge University Press

3.2. Asymptotic reliability of shell finite elements

We recall that our objective is to obtain finite element procedures that behave uniformly well with respect to the thickness parameter, that is, for which the finite element solution $\boldsymbol{Z}_h^\varepsilon$ satisfies an estimate of the type

$$\frac{\|\boldsymbol{Z}^\varepsilon - \boldsymbol{Z}_h^\varepsilon\|_*}{\|\boldsymbol{Z}^\varepsilon\|_*} \leq Ch^k, \tag{3.33}$$

where the norm used remains to be specified. In the light of the above discussion regarding the asymptotic behaviour of shell models, it is natural to require that

(1) in a bending-dominated case, such a uniform estimate should hold in the norm of the displacement space $\boldsymbol{V}$;
(2) in a membrane-dominated case, such a uniform estimate should hold in the membrane energy norm.

We consider a standard finite element procedure obtained by discretizing the variational formulation (3.2), namely the problem:
Find $\boldsymbol{Z}_h^\varepsilon \in \boldsymbol{V}_h$ such that

$$\varepsilon^3 B_F(\boldsymbol{Z}_h^\varepsilon, \boldsymbol{E}) + \varepsilon B_M(\boldsymbol{Z}_h^\varepsilon, \boldsymbol{E}) = L^\varepsilon(\boldsymbol{E}), \quad \forall \boldsymbol{E} \in \boldsymbol{V}_h, \tag{3.34}$$

where $\boldsymbol{V}_h$ denotes the finite element displacement space used. For a membrane-dominated problem we – in fact – need to consider the scaled problem

$$B_M(\boldsymbol{Z}_h^\varepsilon, \boldsymbol{E}) + \varepsilon^2 B_F(\boldsymbol{Z}_h^\varepsilon, \boldsymbol{E}) = G(\boldsymbol{E}), \quad \forall \boldsymbol{E} \in \boldsymbol{V}_h. \tag{3.35}$$

We can then show that we have a uniform convergence property, as proved in Chapelle and Bathe (1998).

Proposition 7. Assume that there exist two interpolation operators $\mathcal{I}_h$ and $\mathcal{J}_h$, defined respectively in $\boldsymbol{V}_M$ and $\boldsymbol{V}$, and both with values in $\boldsymbol{V}_h$, such that

$$\begin{cases} \|\mathcal{I}_h(\boldsymbol{E})\|_M \leq C\|\boldsymbol{E}\|_M, & \forall \boldsymbol{E} \in \boldsymbol{V}_M, \\ \|\mathcal{I}_h(\boldsymbol{E})\|_{\boldsymbol{V}} \leq C\|\boldsymbol{E}\|_{\boldsymbol{V}}, & \forall \boldsymbol{E} \in \boldsymbol{V}, \\ \lim\limits_{h\to 0} \|\boldsymbol{E} - \mathcal{I}_h(\boldsymbol{E})\|_M = 0, & \forall \boldsymbol{E} \in \boldsymbol{V}_M, \end{cases} \tag{3.36}$$

$$\begin{cases} \|\mathcal{J}_h(\boldsymbol{E})\|_{\boldsymbol{V}} \leq C\|\boldsymbol{E}\|_{\boldsymbol{V}}, & \forall \boldsymbol{E} \in \boldsymbol{V}, \\ \lim\limits_{h\to 0} \|\boldsymbol{E} - \mathcal{J}_h(\boldsymbol{E})\|_{\boldsymbol{V}} = 0, & \forall \boldsymbol{E} \in \boldsymbol{V}. \end{cases} \tag{3.37}$$

Then, for any fixed $\varepsilon_{\max} > 0$ we have

$$\lim_{h\to 0} \sup_{\varepsilon \in]0,\varepsilon_{\max}]} \{\|\boldsymbol{Z}^\varepsilon - \boldsymbol{Z}_h^\varepsilon\|_M + \varepsilon \|\boldsymbol{Z}^\varepsilon - \boldsymbol{Z}_h^\varepsilon\|_{\boldsymbol{V}}\} = 0. \tag{3.38}$$

If we consider only the membrane energy norm in this uniform convergence result, this bound is weaker than an estimate of the type (3.33) in the

https://doi.org/10.1017/S0962492901000034 Published online by Cambridge University Press

membrane energy norm. However, this is clearly the best estimate that we can obtain without uniform regularity results on the exact solutions, and such regularity results are not available. We further point out that the interpolation assumptions (3.36) and (3.37) are rather unrestrictive. For example, the Clément operator satisfies these two sets of assumptions when $\boldsymbol{V}_M$ is a Sobolev space on which this operator is properly defined.

By contrast, in a bending-dominated situation, the problem to be considered is instead

$$B_F(\boldsymbol{Z}_h^\varepsilon, \boldsymbol{E}) + \frac{1}{\varepsilon^2} B_M(\boldsymbol{Z}_h^\varepsilon, \boldsymbol{E}) = G(\boldsymbol{E}), \quad \forall \boldsymbol{E} \in \boldsymbol{V}_h. \tag{3.39}$$

The major difficulty associated with this type of finite element formulation is the classical *numerical locking* phenomenon. As is well known from other penalized formulations (*e.g.*, nearly incompressible elasticity, beams, plates), locking occurs at its worst in situations for which

$$\boldsymbol{V}_h \cap \boldsymbol{V}_F = \{\boldsymbol{0}\}. \tag{3.40}$$

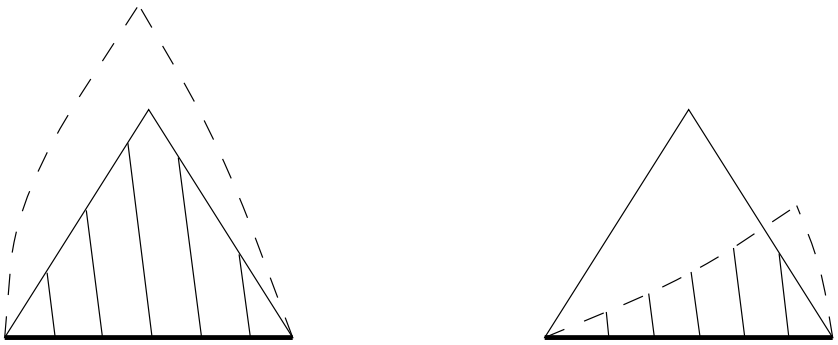
Indeed, Proposition 3 can now be applied with $\boldsymbol{V}_h$ instead of $\boldsymbol{V}$. We thus have that, keeping the finite element subspace (in particular the mesh) fixed, when ε tends to zero the finite element solution $\boldsymbol{Z}_h^\varepsilon$ converges to the solution of the limit problem:
Find $\boldsymbol{Z}_h^0$ in $\boldsymbol{V}_h \cap \boldsymbol{V}_F$ such that

$$B_F(\boldsymbol{Z}_h^0, \boldsymbol{E}) = G(\boldsymbol{E}), \quad \forall \boldsymbol{E} \in \boldsymbol{V}_h \cap \boldsymbol{V}_F, \tag{3.41}$$

and of course the solution of this problem is the zero displacement if (3.40) holds. Even though the thickness is always finite in practice, this implies that no uniform error bound of the type (3.33) holds in this case, and more specifically that, for a given mesh, the finite element solution gets 'smaller and smaller' when the thickness decreases (whereas the exact solution does not vanish). Hence, this is a purely numerical artefact that makes the structure appear stiffer as it gets thinner, which explains the terminology 'numerical locking'. The specific difficulty with shells is that, unlike for beams or plates, the pathological situation expressed by (3.40) is the common rule, as illustrated in the following result, for which we also give the proof because it is simple and illuminating as to how the geometry influences the asymptotic properties (*cf.* also Choï, Palma, Sanchez-Palencia and Vilarino (1998) and Sanchez-Hubert and Sanchez-Palencia (1997) for other results concerning (3.40)).

Proposition 8. Consider a regular hyperbolic shell fixed on some part of its boundary, and a finite element scheme, in the framework of (3.39), in which the displacement components η_1, η_2 and η_3 are approximated using continuous piecewise-polynomial functions. Assume that no element edge in the mesh is part of an asymptotic line. Then (3.40) holds.

https://doi.org/10.1017/S0962492901000034 Published online by Cambridge University Press



(a) (b)

Fig. 3.1. Asymptotic lines and inhibited region for an element

Proof. We will show that, for any inextensional displacement $\boldsymbol{\eta}$, if $\boldsymbol{\eta}$ is zero on some edge of any element of the mesh, then $\boldsymbol{\eta}$ is identically zero over the whole element. This being granted, the result is immediately obtained by 'propagating' the zero displacements from the boundary conditions to the whole domain.

Consider an arbitrary element of the mesh, with $\boldsymbol{\eta}$ set to zero on any of its edges. Then we have two possibilities: *either*

(a) the lattice of asymptotic lines originating from this edge covers the element completely (as in Figure 3.1(a)) and the conclusion directly follows from Proposition 6; *or*

(b) the element is only partially covered (Figure 3.1(b)), but in this case we still have $\eta_1 = \eta_2 = \eta_3 = 0$ on a part of the nonzero area of the element. Recalling that the displacement components are given by polynomial functions, this implies that they are zero over the whole element. □

In order to make the statement of this property simpler, we have assumed that no single element edge corresponds to an asymptotic curve. It is obvious, however, that this result carries over to any case in which the same propagation technique can be applied, which is much more general. A practical consequence of this discussion is that, when using benchmark problems to detect locking phenomena in shells numerically, we should not align the mesh with the asymptotic lines of the mid-surface when such lines exist, in order to avoid inhibiting the locking mechanism identified in the above proof. This holds in particular for *cylindrical test problems* for which the (very strong) temptation to align the mesh along the axis should definitely

https://doi.org/10.1017/S0962492901000034 Published online by Cambridge University Press

be resisted if one wants to draw conclusions of somewhat general significance (note that, in industrial computations, aligning meshes along lines of specific geometric properties is impossible in general).

We further emphasize that Proposition 8 reveals a significant difference between finite element methods for shells and for other structures. For beams and plates, it is indeed always possible to avoid (3.40) by raising the polynomial degrees of the discretization spaces; see in particular Arnold (1981). Here our argument is independent of the polynomial degree, hence *locking always occurs using displacement-based finite element formulations.* But of course, for a given thickness, the errors in the solution may be acceptably small if the order of the polynomials is sufficiently high and the mesh is sufficiently fine.

In order to circumvent the locking phenomenon, it is now classical to resort to *mixed formulations*, in which an additional unknown – corresponding to the 'delinquent' term of the energy – is introduced; see Brezzi and Fortin (1991) and Bathe (1996). For example, for Reissner–Mindlin plates this additional unknown corresponds to the shear stress. For shell formulations, it is thus natural to introduce the membrane stresses (and the shear stresses for Reissner–Mindlin-type models) as auxiliary unknowns. For instance, for the Koiter shell model the additional unknown is the membrane stress tensor, namely the tensor with contravariant components

$$m^{\alpha\beta} = \frac{1}{\varepsilon^2} a^{\alpha\beta\sigma\tau} \gamma_{\sigma\tau}(\boldsymbol{\zeta}). \tag{3.42}$$

If we symbolically denote by $\boldsymbol{\Sigma}^\varepsilon$ the group of additional stress unknowns, and by $\boldsymbol{\Xi}$ the corresponding test function, the mixed formulation equivalent to (3.12) then reads

$$\begin{cases} B_F(\boldsymbol{Z}^\varepsilon, \boldsymbol{E}) + M(\boldsymbol{E}, \boldsymbol{\Sigma}^\varepsilon) = G(\boldsymbol{E}), & \forall \boldsymbol{E} \in \boldsymbol{V}, \\ M(\boldsymbol{Z}^\varepsilon, \boldsymbol{\Xi}) - \varepsilon^2 D(\boldsymbol{\Sigma}^\varepsilon, \boldsymbol{\Xi}) = 0, & \forall \boldsymbol{\Xi} \in \boldsymbol{L}^2, \end{cases} \tag{3.43}$$

where the second equation expresses the stress–strain relationship for the additional unknowns, and $\boldsymbol{L}^2$ denotes the product space obtained by taking $L^2(\omega)$ for each component of the stress term. By construction, $D(\boldsymbol{\Xi}, \boldsymbol{\Xi})^{1/2}$ defines a norm which is equivalent to the L^2-norm, and the mixed bilinear form M is continuous over $\boldsymbol{V} \times \boldsymbol{L}^2$; see, *e.g.*, Arnold and Brezzi (1997). Then, both fields (displacements and stresses) are discretized in the finite element procedure. In general, discontinuous shape functions are used for the stresses, in order to allow the elimination of the stress degrees of freedom at the element level. The resulting finite element formulation can then be written as

$$B_F(\boldsymbol{Z}_h^\varepsilon, \boldsymbol{E}) + \frac{1}{\varepsilon^2} B_M^h(\boldsymbol{Z}_h^\varepsilon, \boldsymbol{E}) = G(\boldsymbol{E}), \quad \forall \boldsymbol{E} \in \boldsymbol{V}_h, \tag{3.44}$$

https://doi.org/10.1017/S0962492901000034 Published online by Cambridge University Press

where B_M^h is a bilinear form that 'resembles B_M', but for which the constraint $B_M^h(\boldsymbol{E},\boldsymbol{E}) = 0$ is 'more easily satisfied' for finite element displacements than $B_M(\boldsymbol{E},\boldsymbol{E}) = 0$. Note that, from this point of view, this strategy is fairly close to the engineering-based idea of reduced integration. In fact, in some cases it has been possible to substantiate some previously proposed reduced-integration schemes using the theory of mixed methods (*cf.*, *e.g.*, Lyly (2000)). When the analysis of the mixed formulation can be achieved, it indeed provides a proof that uniform convergence with respect to ε holds (in the norm of $\boldsymbol{V}$). This analysis, however, relies on a crucial *inf-sup condition* which can be written in the general form

$$\sup_{\boldsymbol{E}\in\boldsymbol{V}_h} \frac{M(\boldsymbol{E},\boldsymbol{\Xi})}{\|\boldsymbol{E}\|_{\boldsymbol{V}}} \geq \gamma \sup_{\boldsymbol{E}\in\boldsymbol{V}} \frac{M(\boldsymbol{E},\boldsymbol{\Xi})}{\|\boldsymbol{E}\|_{\boldsymbol{V}}}, \qquad \forall \boldsymbol{\Xi} \in \boldsymbol{S}_h, \tag{3.45}$$

where $\boldsymbol{S}_h$ denotes the discrete stress space and γ is a strictly positive constant independent of h and ε. Defining the seminorm

$$|\boldsymbol{\Xi}|_{\boldsymbol{S}} = \sup_{\boldsymbol{E}\in\boldsymbol{V}} \frac{M(\boldsymbol{E},\boldsymbol{\Xi})}{\|\boldsymbol{E}\|_{\boldsymbol{V}}}, \tag{3.46}$$

we have the equivalent – more classical – expression of the inf-sup condition

$$\inf_{\substack{\boldsymbol{\Xi}\in\boldsymbol{S}_h \\ |\boldsymbol{\Xi}|_{\boldsymbol{S}}\neq 0}} \sup_{\boldsymbol{E}\in\boldsymbol{V}_h} \frac{M(\boldsymbol{E},\boldsymbol{\Xi})}{|\boldsymbol{\Xi}|_{\boldsymbol{S}}\|\boldsymbol{E}\|_{\boldsymbol{V}}} \geq \gamma > 0. \tag{3.47}$$

This inf-sup condition requires a deep correlation between the displacement and stress finite element spaces in order to be fulfilled. For shell formulations, the problem of finding a couple of displacement/stress finite element spaces in order to satisfy the corresponding inf-sup condition is still open (*cf.* Arnold and Brezzi (1997) for an attempt in this direction).

In the case of nearly incompressible elasticity where locking also arises, owing to the kinematic constraint introduced by the incompressibility condition, a numerical procedure – called the *inf-sup test* – has been introduced in Chapelle and Bathe (1993) to test whether the inf-sup condition is satisfied without resorting to an actual mathematical proof. This procedure has been shown to give very reliable results (*i.e.*, by clearly indicating whether the condition is satisfied or not) on numerous finite element procedures for which theoretical results where available; see also Iosilevich, Bathe and Brezzi (1997) for plate formulations. A similar test has been devised and used in Bathe, Iosilevich and Chapelle (2000) for shells. The MITC shell elements (MITC4, MITC9 and MITC16 elements, *cf.* Bathe and Dvorkin (1986) and Bucalem and Bathe (1993)), which are based on a mixed formulation, have passed this numerical testing procedure, whereas the corresponding standard finite elements (which are also called *displacement-based* methods to distinguish them from mixed methods) have all failed as expected. How-

https://doi.org/10.1017/S0962492901000034 Published online by Cambridge University Press

ever, the absence of theoretical results pertaining to shell inf-sup conditions does not allow a thorough validation of this test at present. Moreover, two other reasons make it difficult to advocate the shell inf-sup test as strongly as for nearly incompressible elasticity.

(1) The dramatic dependence of the shell behaviour on the geometry (and the boundary conditions), which implies that many configurations should probably be considered in order to reach an acceptable level of confidence (only one configuration was used for nearly incompressible elasticity).

(2) The inf-sup condition that the test is based upon is in fact stronger than the inf-sup condition corresponding to the shell mixed formulation, which means that a given finite element procedure could satisfy the actual inf-sup condition and yet fail in the numerical test.

Given the considerable difficulty in proving an inf-sup condition for shell finite elements, another interesting idea, proposed and analysed in Bramble and Sun (1997), is to relax the inf-sup condition while tolerating some degree of non-uniformity in the convergence of the approximate solutions; namely, a mixed method is used for which a stability condition weaker than the inf-sup condition (3.45) is shown to hold, and a uniform error estimate is then obtained *under the condition*

$$h \leq C\sqrt{\varepsilon}. \tag{3.48}$$

This means that locking should not appear unless a very small thickness (or a coarse mesh) is used. However, a thorough numerical testing of this finite element procedure is lacking, as regards locking as well as other difficulties featured by mixed finite elements for shells (see below).

Finally, as regards the mathematical analysis of the locking of shell problems, to the best of our knowledge the only shell finite element method for which an analysis *valid for general geometries* has provided a uniform error estimate is the method given in Chapelle and Stenberg (1998). This method corresponds to a *mixed–stabilized* formulation in which additional stabilizing terms are added to the mixed formulation in order to bypass the inf-sup condition.

In the framework of shell models, mixed formulations feature another serious difficulty, which is that they are clearly tailored to the approximation of a problem in which a constraint is enforced by penalization. But for shell problems to fall into that category, according to our above discussion the asymptotic behaviour must be of the bending-dominated type. On the other hand, if the problem solved using a mixed method happens to be of the membrane-dominated type, instead of (3.44) we in fact need to consider

$$B_M^h(\boldsymbol{Z}_h^\varepsilon, \boldsymbol{E}) + \varepsilon^2 B_F(\boldsymbol{Z}_h^\varepsilon, \boldsymbol{E}) = G(\boldsymbol{E}), \quad \forall \boldsymbol{E} \in \boldsymbol{V}_h. \tag{3.49}$$

https://doi.org/10.1017/S0962492901000034 Published online by Cambridge University Press

Hence, compared to equation (3.35) satisfied by the exact solution, the mixed formulation leads to a perturbation of the *leading term* of the formulation. Therefore, convergence (and in particular uniform convergence) cannot be expected in this case unless the *consistency* of B_M^h with respect to B_M is strictly controlled. This condition is very difficult to enforce, in particular because mixed methods are not designed to that purpose. As a matter of fact, for the above-mentioned mixed–stabilized scheme that works well in bending-dominated cases, uniform convergence is not obtained in membrane-dominated situations.

Therefore, it appears that we are 'trapped' in a dilemma caused by the dramatic discrepancy between the two major asymptotic states of shell problems. Displacement-based finite elements work well in membrane-dominated situations but are subject to numerical locking in bending-dominated situations, in general. On the other hand, if we try to 'fix' the bending-dominated behaviour by using mixed methods (or some kind of reduced integration strategy), there is a major risk of seriously deteriorating the numerical solution in membrane-dominated cases. As a matter of fact, we do not know of any shell finite element procedure that would have been proved to work well in both regimes.

3.3. Guidelines for assessing and improving the reliability of shell finite elements

Whereas the complete mathematical analysis required to design and justify a general uniformly convergent finite element method for shell problems still seems out of reach, we believe that it is crucial, in this reliability quest, to combine the insight provided by the analysis of the mathematical models and the elements of analysis available on their discretizations on the one hand, with extensive numerical testing on the other hand. In this interaction, *benchmarks* are both an essential interface and an invaluable means of assessing the performance and the reliability of shell finite element methods, hence also to improve these methods.

Of course, in order to provide a rigorous and meaningful assessment tool, benchmarks must be very carefully chosen, and properly used. To that purpose, some detailed guidelines are given in Chapelle and Bathe (1998), which rely on the following principles.

- A basic set of benchmarks must contain instances of the two fundamental categories of asymptotic behaviour of shell structures.
- Several geometries must be considered, since the asymptotic behaviour is highly sensitive on the geometry of the mid-surface (for example, a set of benchmarks only based on cylinders is not satisfactory).
- Numerical computations must be performed and reported upon for several values of h (since we are concerned with the whole convergence

https://doi.org/10.1017/S0962492901000034 Published online by Cambridge University Press

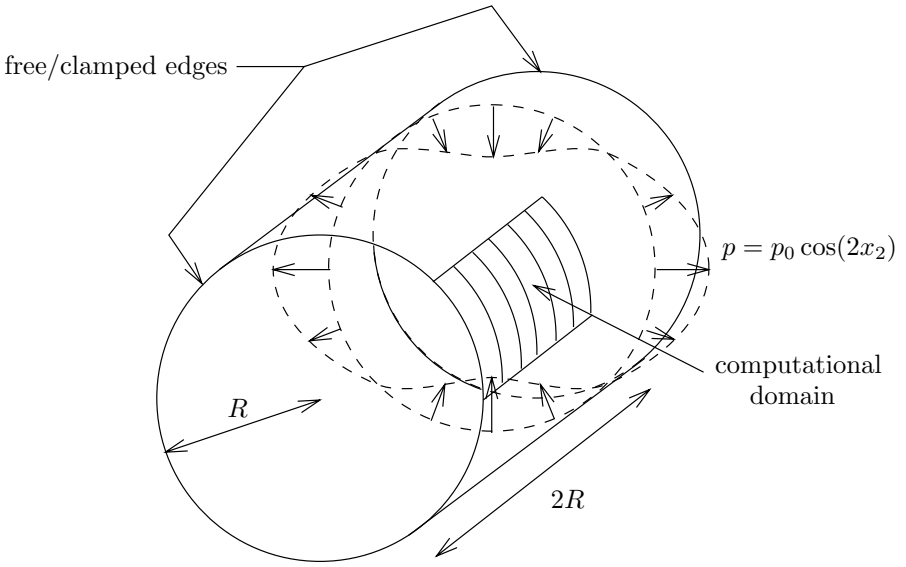


Fig. 3.2. Cylinder loaded by periodic pressure

behaviour and not only with the accuracy in one specific instance) and for several values of ε (in order to assess the robustness of the convergence with respect to this parameter).

In Chapelle and Bathe (1998), a basic set of benchmarks is also proposed based on these principles. It consists of the following test problems.

Circular cylinder loaded by periodic pressure. (See Figure 3.2.) Depending on the boundary conditions we can obtain either one of the two main asymptotic behaviour types (bending-dominated behaviour if both ends are left free, well-posed membrane-dominated behaviour if both ends are clamped). This problem was originally proposed in Pitkäranta, Leino, Ovaskainen and Piila (1995) which also presented a procedure for obtaining numerical solutions of arbitrary accuracy.[1]

Partly clamped hyperbolic paraboloid. The shell shown in Figure 3.3 is clamped on one side and loaded, *e.g.*, by self weight. It can be shown that pure bending is not inhibited; *cf.* Chapelle and Bathe (1998). We do not have an analytical solution for this problem (see Choï (1999) where the exact solution of the limit problem is analysed), but we can use reference solutions obtained with a very fine mesh to compute error measures.

[1] The values of displacements and deformation energies given in Pitkäranta *et al.* (1995) should be multiplied by $(1-\nu^2)$ and $(1-\nu^2)^2$, respectively.

https://doi.org/10.1017/S0962492901000034 Published online by Cambridge University Press

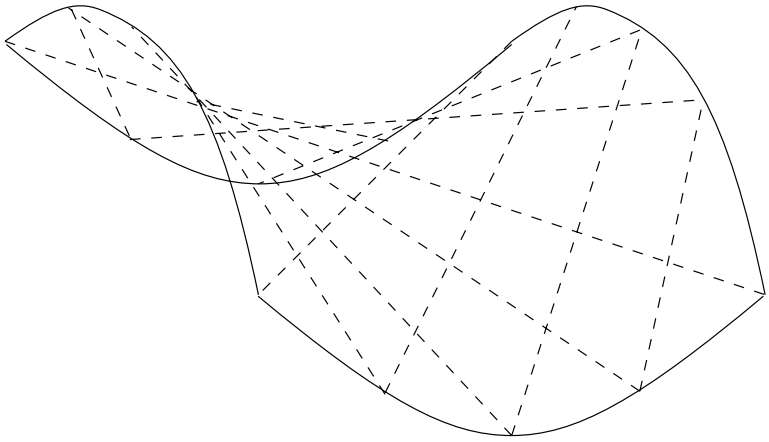


Fig. 3.3. Hyperbolic paraboloid

Clamped hemispherical cap. It can be shown that pure bending is inhibited for this problem (as a matter of fact, non-inhibited pure bending is obtained for a hemispherical cap only when the boundary is completely free; see Sanchez-Hubert and Sanchez-Palencia (1997), and also Chapelle and Bathe (1998)). If we choose an axisymmetric loading such as the one shown in Figure 3.4, we can compare the results of the shell analysis with the results of some (reliable) axisymmetric analysis scheme.

We also emphasize that a deep insight into the behaviour of the exact solutions is an essential prerequisite in the assessment procedure, that is, in the proper use of benchmarks. A particularly important feature of these solutions is the development of boundary layers which vary in amplitude and width when the thickness of the shell varies. If these boundary layers are not properly taken into account in the choice of the discretization scheme (in particular by refining the mesh when and where appropriate), they can strongly affect the convergence behaviour and induce wrong conclusions in the reliability assessment. This insight, available for plates (see, *e.g.*, Häggblad and Bathe (1990), Arnold and Falk (1996), Dauge and Yosibash (2000)), is now becoming available for shells also through some more recent works (Pitkäranta, Matache and Schwab 1999, Karamian, Sanchez-Hubert and Sanchez-Palencia 2000).

Once a good set of benchmarks has been selected, it is crucial to measure the error made in the numerical computations by using proper error measures. We now review and evaluate some possible choices, including those currently most widely used.

https://doi.org/10.1017/S0962492901000034 Published online by Cambridge University Press

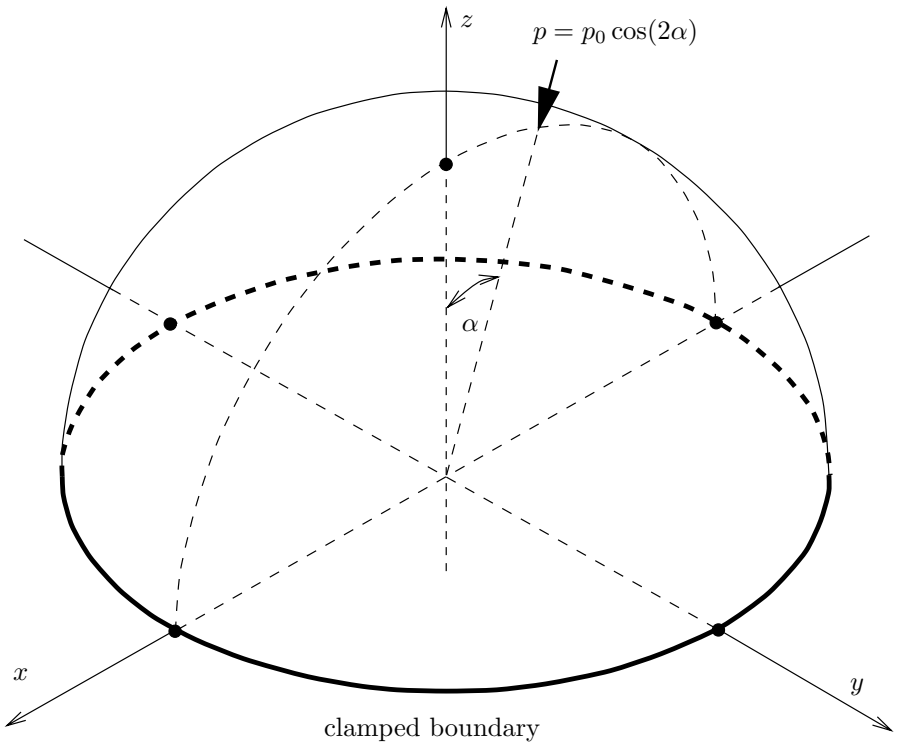


Fig. 3.4. Hemispherical shell under axisymmetric loading

(1) Pointwise displacements. This error measure is probably the most extensively used, especially in the engineering literature. It is, however, likely to be misleading, since the pointwise convergence of finite element methods is not guaranteed, in general.

(2) Energy norm, namely $[\varepsilon^2 B_F(\boldsymbol{E}, \boldsymbol{E}) + B_M(\boldsymbol{E}, \boldsymbol{E})]^{1/2}$ (note that we can scale the energy by any given power of ε since we are concerned with relative errors). This cannot be a good choice, since it is the norm in which the displacement-based finite element solution is the best approximation, whereas this solution locks in bending-dominated situations.

(3) Modified energy norm, namely $[\varepsilon^2 B_F(\boldsymbol{E}, \boldsymbol{E}) + B_M^h(\boldsymbol{E}, \boldsymbol{E})]^{1/2}$. This choice is advocated in Malinen and Pitkäranta (2000), in particular. Its major drawback, beside the fact that its use with the exact solution (or any reference solution) is delicate (since the B_M^h-form is usually tailored to one particular discretization), is that the use of a non-physical modification of the energy makes it difficult to interpret convergence in this norm.

https://doi.org/10.1017/S0962492901000034 Published online by Cambridge University Press

(4) Energy variation, namely $|\mathcal{E} - \mathcal{E}_h|$ where $\mathcal{E}$ is the energy that corresponds to the exact (or reference) solution, namely

$$\mathcal{E} = \varepsilon^2 B_F(\boldsymbol{Z}^\varepsilon, \boldsymbol{Z}^\varepsilon) + B_M(\boldsymbol{Z}^\varepsilon, \boldsymbol{Z}^\varepsilon), \tag{3.50}$$

and $\mathcal{E}_h$ the energy of the finite element solution, namely

$$\mathcal{E}_h = \varepsilon^2 B_F(\boldsymbol{Z}_h^\varepsilon, \boldsymbol{Z}_h^\varepsilon) + B_M(\boldsymbol{Z}_h^\varepsilon, \boldsymbol{Z}_h^\varepsilon) \tag{3.51}$$

for displacement-based methods and

$$\mathcal{E}_h = \varepsilon^2 B_F(\boldsymbol{Z}_h^\varepsilon, \boldsymbol{Z}_h^\varepsilon) + B_M^h(\boldsymbol{Z}_h^\varepsilon, \boldsymbol{Z}_h^\varepsilon) \tag{3.52}$$

for mixed methods. For displacement-based methods, it can be shown that this measure equals the square of the error in the energy norm, but this does not hold for mixed methods, which makes the interpretation of this indicator very difficult (see also Malinen and Pitkäranta (2000)).

(5) Asymptotic convergence norms, namely – as discussed in the introduction of this section – the norms in which exact solutions are shown to converge to limit solutions, that is, the norm of the displacement space for bending-dominated problems and the membrane energy norm for membrane-dominated problems. For practical purposes the membrane energy norm can be directly computed using its definition (and the corresponding stiffness matrices). For the norm of the displacement space (typically a combination of Sobolev norms) it is more convenient to use an equivalent norm constructed with the deformation energy, for example $[L^2 B_F(\boldsymbol{E}, \boldsymbol{E}) + B_M(\boldsymbol{E}, \boldsymbol{E})]^{1/2}$ where L is a characteristic dimension of the structure (the diameter, for instance). Note that, when using general shell elements, these computations are not straightforward since the membrane and bending energies are combined in the basic shell model. However, as a consequence of our above discussion (*cf.* Section 3.1), since the Naghdi model is asymptotically equivalent we can use the corresponding energy expressions (and stiffness matrices) to compute adequate norms.

Using the norms in which asymptotic convergence is obtained for the exact solutions, it is then natural to seek finite element procedures for which uniformly decreasing errors can be measured on benchmarks such as those proposed above, when boundary layers (namely, the 'nonsmooth part' of the exact solutions) are properly resolved. Indeed, for a displacement-based finite element procedure used in a membrane-dominated case it can be shown that (see Chapelle and Bathe (1998))

$$\begin{aligned} \|\boldsymbol{Z}^\varepsilon - \boldsymbol{Z}_h^\varepsilon\|_M + \varepsilon \|\boldsymbol{Z}^\varepsilon - \boldsymbol{Z}_h^\varepsilon\|_{\boldsymbol{V}} \\ \leq C \inf_{\boldsymbol{E} \in \boldsymbol{V}_h} \{\|\boldsymbol{Z}^\varepsilon - \boldsymbol{E}\|_M + \varepsilon \|\boldsymbol{Z}^\varepsilon - \boldsymbol{E}\|_{\boldsymbol{V}}\}, \end{aligned} \tag{3.53}$$

https://doi.org/10.1017/S0962492901000034 Published online by Cambridge University Press

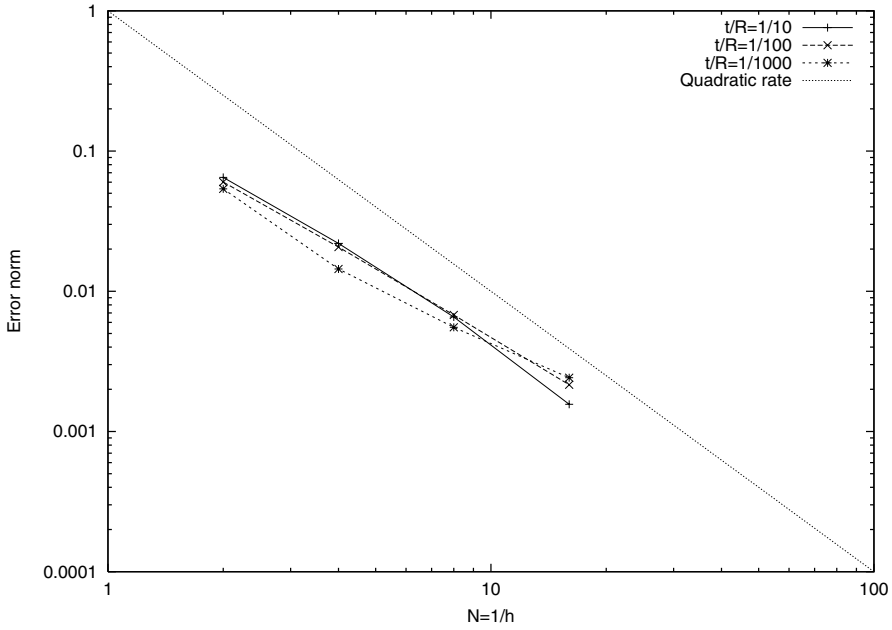


Fig. 3.5. Clamped cylinder: adapted mesh, membrane norm

which shows that a displacement-based finite element procedure is *uniformly optimal* with respect to ε for the norm $\|\cdot\|_M + \varepsilon\|\cdot\|_{\boldsymbol{V}}$. Therefore, if the mesh is refined so that the boundary layers of a given test problem are properly resolved for this norm, uniform optimal convergence is obtained. This is illustrated in Figures 3.5–3.7, where the case of a clamped circular cylinder is considered (as described in Figure 3.2); see Chapelle, Oliveira and Bucalem (200x). The Naghdi model is used, and Q2 displacement-based elements are employed to discretize the problem. Figure 3.5 shows the convergence curves obtained for the membrane norm and for decreasing values of ε (t denotes the actual thickness of the shell, namely 2ε) when as many layers of elements are used within the layer of width $\sqrt{\varepsilon}$ along the boundaries (*i.e.*, the boundary layers) as in the rest of the domain. This can be shown to be the correct way to resolve the boundary layers; see Pitkäranta *et al.* (1995). We can see that the convergence rate is optimal for all values of the thickness, and the convergence behaviour is not particularly sensitive to the value of ε. By contrast, if no particular treatment of the boundary layers is applied, we obtain the convergence curves displayed in Figure 3.6 where some significant sensitivity with respect to ε is observed. Also, if the original norm of $\boldsymbol{V}$ is used instead of the membrane norm (Figure 3.7) we again detect some marked sensitivity. All these numerical results are clearly consistent with equation (3.53).

https://doi.org/10.1017/S0962492901000034 Published online by Cambridge University Press

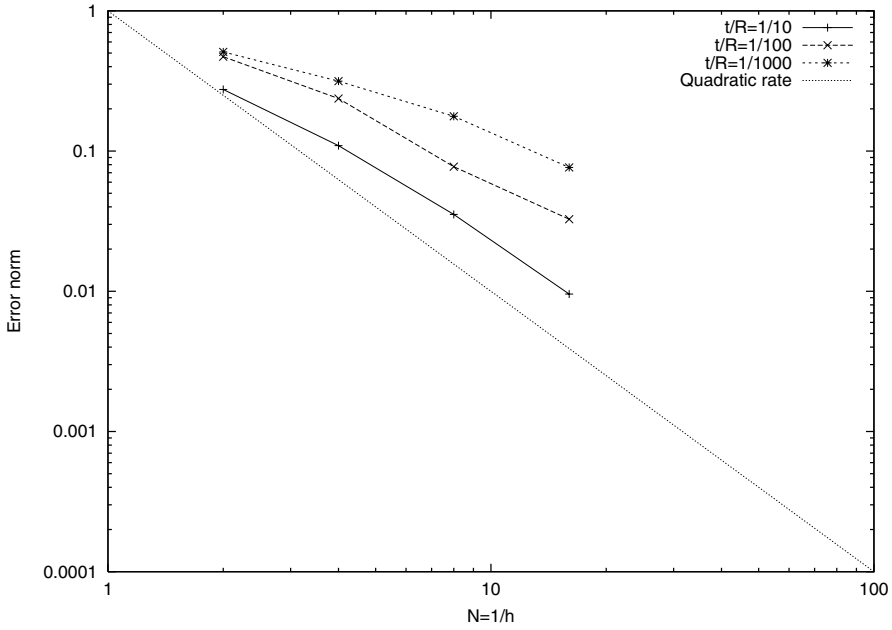


Fig. 3.6. Clamped cylinder: non-adapted mesh, membrane norm

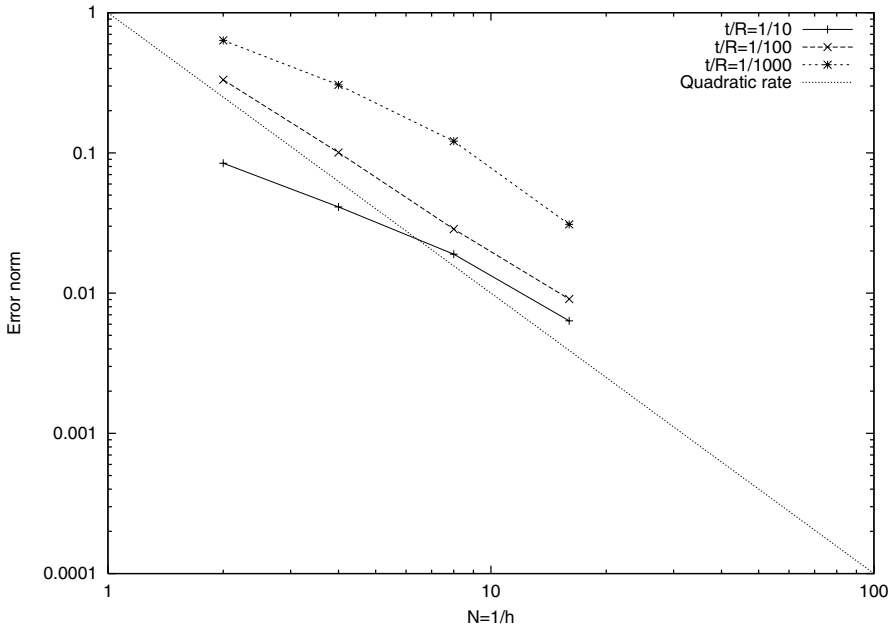


Fig. 3.7. Clamped cylinder: adapted mesh, original norm

https://doi.org/10.1017/S0962492901000034 Published online by Cambridge University Press

Likewise, for bending-dominated problems classical results for mixed formulations show that, when the inf-sup condition is satisfied, we have the following optimal error bound (see Brezzi and Fortin (1991)):

$$\|\boldsymbol{Z}^{\varepsilon} - \boldsymbol{Z}_h^{\varepsilon}\|_{\boldsymbol{V}} + |\boldsymbol{\Sigma}^{\varepsilon} - \boldsymbol{\Sigma}_h^{\varepsilon}|_{\boldsymbol{S}} \leq C \inf_{\substack{\boldsymbol{E}\in\boldsymbol{V}_h \\ \boldsymbol{\Xi}\in\boldsymbol{S}_h}} \{\|\boldsymbol{Z}^{\varepsilon} - \boldsymbol{E}\|_{\boldsymbol{V}} + |\boldsymbol{\Sigma}^{\varepsilon} - \boldsymbol{\Xi}|_{\boldsymbol{S}}\}. \quad (3.54)$$

Of course, as previously mentioned, we do not know of any shell finite element procedure that is proven to satisfy the inf-sup condition. Note, however, that a procedure which passes the inf-sup test on a given test problem automatically satisfies the estimate (3.54) *for this same test problem and on the sequence of meshes used for the inf-sup test* (as it is the inf-sup *values* that enter in the bounding constants). Moreover, the estimate (3.54) is very useful for determining how the meshes should be refined in order to ascertain uniformly converging errors in the numerical results obtained with finite element schemes that 'would satisfy' the inf-sup condition (hence locking-free finite elements), even though this inf-sup condition cannot be proven. Namely, the regularity of the stresses also needs to be considered to control the error in the seminorm $|\cdot|_{\boldsymbol{S}}$ (note that this seminorm is always bounded by the L^2-norm – *cf.* Chapelle and Stenberg (1998)).

Finally, we emphasize that all the above-proposed benchmarks are based on problems for which a well-defined asymptotic limit exists, and more specifically for which the asymptotic behaviour is either membrane-dominated or bending-dominated. As previously discussed, other types of asymptotic behaviour (as defined in Section 3.1) do exist, and in particular in cases when pure bending is inhibited and '$G \notin (\boldsymbol{V}_M)'$'; see in particular Pitkäranta and Sanchez-Palencia (1997) and Pitkäranta *et al.* (1995) for examples. In these cases, however, it does not seem possible to identify a norm for which an asymptotic limit exists, hence it is difficult to see what kind of uniform convergence could be sought in finite element solutions. This is why the use of such problems cannot be recommended to assess the reliability of finite element procedures. We point out that the 'Scordelis–Lo roof' (for which the geometry and the boundary conditions are defined in Figure 3.8, and the loading corresponds to self-weight), which appears to be one of the most widely used test problems in the engineering literature, belongs to this category, as it can be shown that it corresponds to a situation of inhibited pure bending with '$G \notin (\boldsymbol{V}_M)'$'; see Chapelle and Bathe (1998) (in fact, it is the loading in the vicinity of the free boundaries which causes this difficulty). Nevertheless, some recent works have shown that in some cases (more specifically when the shell mid-surface is parabolic or hyperbolic) it is possible to split the solution into several components, namely a smooth part (in which the membrane energy is asymptotically dominant as in membrane-dominated situations) and a singular part, where the singular part consists of strong boundary layers or of 'generalized layers' that lie along asymp-

https://doi.org/10.1017/S0962492901000034 Published online by Cambridge University Press

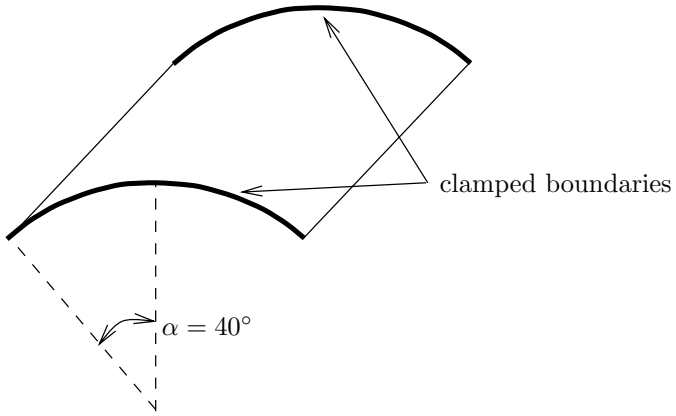


Fig. 3.8. Scordelis–Lo roof

totic lines of the surface; see Pitkäranta *et al.* (1999) and also Karamian *et al.* (2000). Moreover, the displacements that develop in these layers appear to be very similar to pure bending displacements. Even though more analysis is still needed, these recent results give hope that finite element procedures which would perform well (*i.e.*, converge uniformly) in bending-dominated and membrane-dominated situations would also perform well in these more complex situations, that is, converge uniformly for each of the above-mentioned components separately.

Acknowledgement

The author is particularly indebted to Professor Klaus-Jürgen Bathe, as many ideas and results presented in this article originated from a fruitful collaboration with him, which is attested by the joint publications listed in the references.

REFERENCES

S. Ahmad, B. M. Irons and O. C. Zienkiewicz (1970), 'Analysis of thick and thin shell structures by curved finite elements', *Internat. J. Numer. Methods Eng.* **2**, 419–451.

J. L. Akian and E. Sanchez-Palencia (1992), 'Approximation de coques élastiques minces par facettes plane: Phénomènes de blocage membranaire', *C. R. Acad. Sci. Paris, Sér. I* **315**, 363–369.

D. N. Arnold (1981), 'Discretization by finite elements of a model parameter dependent problem', *Numer. Math.* **37**, 405–421.

D. N. Arnold and F. Brezzi (1997), 'Locking-free finite element methods for shells', *Math. Comp.* **66**, 1–14.

D. N. Arnold and R. S. Falk (1996), 'Asymptotic analysis of the boundary layer for the Reissner–Mindlin plate model', *SIAM J. Math. Anal.* **27**, 486–514.

https://doi.org/10.1017/S0962492901000034 Published online by Cambridge University Press

C. Baiocchi and C. Lovadina (200x), A shell classification by interpolation, To appear.
Y. Başar and W. B. Krätzig (1989), ' A consistent shell theory for finite deformations', *Acta Mech.* **76**, 73–87.
K. J. Bathe (1996), *Finite Element Procedures*, Prentice-Hall, Englewood Cliffs, NJ.
K. J. Bathe and D. Chapelle (200x), *The Finite Element Analysis of Shells.* To appear.
K. J. Bathe and E. N. Dvorkin (1986), 'A formulation of general shell elements: The use of mixed interpolation of tensorial components', *Internat. J. Numer. Methods Eng.* **22**, 697–722.
K. J. Bathe, A. Iosilevich and D. Chapelle (2000), 'An inf-sup test for shell finite elements', *Comput. Structures* **75**, 439–456.
J. L. Batoz and G. Dhatt (1992), *Modélisation des Structures par Eléments Finis, Vol. 3: Coques*, Hermes, Paris.
M. Bernadou (1996), *Finite Element Methods for Thin Shell Problems*, Wiley.
M. Bernadou and P. G. Ciarlet (1976), Sur l'ellipticité du modèle linéaire de coques de W. T. Koiter, in *Computing Methods in Applied Sciences and Engineering* (R. Glowinski and J. L. Lions, eds), Vol. 134 of *Lecture Notes in Economics and Mathematical Systems*, Springer, Heidelberg, pp. 89–136.
M. Bernadou, Y. Ducatel and P. Trouvé (1988), 'Approximation of a circular cylindrical shell by Clough–Johnson flat plate finite elements', *Numer. Math.* **52**, 187–217.
M. Bernadou, P. G. Ciarlet and B. Miara (1994), 'Existence theorems for two-dimensional linear shell theories', *J. Elasticity* **34**, 111–138.
M. Bischoff and E. Ramm (1997), 'Shear deformable shell elements for large strains and rotations', *Internat. J. Numer. Methods Eng.* **40**, 4427–4449.
A. Blouza, F. Brezzi and C. Lovadina (1999), 'Sur la classification des coques linéairement élastiques', *C. R. Acad. Sci. Paris, Sér. I* **328**, 831–836.
J. Bramble and T. Sun (1997), 'A locking-free finite element method for Naghdi shells', *J. Comput. Appl. Math.* **89**, 119–133.
F. Brezzi and M. Fortin (1991), *Mixed and Hybrid Finite Element Methods*, Springer.
M. L. Bucalem and K. J. Bathe (1993), 'Higher-order MITC general shell elements', *Internat. J. Numer. Methods Eng.* **36**, 3729–3754.
D. Chapelle and K. J. Bathe (1993), 'The inf-sup test', *Comput. Structures* **47**, 537–545.
D. Chapelle and K. J. Bathe (1998), 'Fundamental considerations for the finite element analysis of shell structures', *Comput. Structures* **66**, 19–36.
D. Chapelle and K. J. Bathe (2000), 'The mathematical shell model underlying general shell elements', *Internat. J. Numer. Methods Eng.* **48**, 289–313.
D. Chapelle, D. L. Oliveira, and M. L. Bucalem (200x), 'On the reliability of MITC shell finite elements based on Naghdi's model'. To appear.
D. Chapelle and R. Stenberg (1998), 'Stabilized finite element formulations for shells in a bending dominated state', *SIAM J. Numer. Anal.* **36**, 32–73.
D. Chenais and J. C. Paumier (1994), 'On the locking phenomenon for a class of elliptic problems', *Numer. Math.* **67**, 427–440.

https://doi.org/10.1017/S0962492901000034 Published online by Cambridge University Press

D. Choï (1999), 'Computations on thin non-inhibited hyperbolic elastic shells: Benchmarks for membrane locking', *Math. Meth. Appl. Sci.* **22**, 1293–1321.

D. Choï, F. Palma, E. Sanchez-Palencia and M. Vilarino (1998), 'Membrane locking in the finite element computation of very thin elastic shells', *Modélisation Mathématique et Analyse Numérique* **32**, 131–152.

P. G. Ciarlet (1978), *The Finite Element Method for Elliptic Problems*, North-Holland.

P. G. Ciarlet (2000), *Mathematical Elasticity, Volume III: Theory of Shells*, North-Holland.

P. G. Ciarlet (2001), 'Mathematical modelling of linearly elastic shells', in *Acta Numerica*, Vol. 10, Cambridge University Press, pp. 103–214.

M. Dauge and Z. Yosibash (2000), 'Boundary layer realization in thin elastic 3D domains and 2D hierarchic plate models', *Internat. J. Solids Structures* **37**, 2443–2471.

M. Delfour (1998), Intrinsic differential geometric methods in the asymptotic analysis of linear thin shells, in *Boundaries, Interfaces and Transitions* (M. Delfour, ed.), *CRM Proceedings & Lecture Notes*, American Mathematical Society, Providence, RI, pp. 19–90.

B. Häggblad and K. J. Bathe (1990), 'Specifications of boundary conditions for Reissner/Mindlin plate bending finite elements', *Internat. J. Numer. Methods Eng.* **30**, 981–1011.

A. Iosilevich, K. J. Bathe and F. Brezzi (1997), 'On evaluating the inf-sup condition for plate bending elements', *Internat. J. Numer. Methods Eng.* **40**, 3639–3663.

B. M. Irons and S. Ahmad (1980), *Techniques of Finite Elements*, Wiley, London.

P. Karamian, J. Sanchez-Hubert and E. Sanchez-Palencia (2000), 'A model problem for boundary layers of thin elastic shells', *Math. Modelling Numer. Anal.* **34**, 1–30.

W. T. Koiter (1966), 'On the nonlinear theory of thin elastic shells', *Proc. Kon. Ned. Akad. Wetensch.* **B69**, 1–54.

J. L. Lions (1973), *Perturbations Singulières dans les Problèmes aux Limites et en Contrôle Optimal*, Springer.

M. Lyly (2000), 'On the connection between some linear triangular Reissner–Mindlin plate bending elements', *Numer. Math.* **85**, 77–107.

M. Malinen (2000), On geometrically incompatible bilinear shell elements and classical shell models, Research Report TKK-Lo-30, Helsinki University of Technology, Laboratory for Mechanics of Materials.

M. Malinen and J. Pitkäranta (2000), A benchmark study of reduced-strain shell finite elements: Quadratic schemes. *Internat. J. Numer. Methods Eng.* **48** 1637–1671.

R. Mindlin (1951), 'Influence of rotary inertia and shear on flexural motion of isotropic elastic plates', *J. Appl. Mech.* **18**, 31–38.

P. M. Naghdi (1963), Foundations of elastic shell theory, in *Progress in Solid Mechanics*, Vol. 4, North-Holland, pp. 1–90.

J. Pitkäranta (1992), 'The problem of membrane locking in finite element analysis of cylindrical shells', *Numer. Math.* **61**, 523–542.

J. Pitkäranta and E. Sanchez-Palencia (1997), 'On the asymptotic behaviour

https://doi.org/10.1017/S0962492901000034 Published online by Cambridge University Press

of sensitive shells with small thickness', *C. R. Acad. Sci. Paris, Sér. IIb* **325**, 127–134.

J. Pitkäranta, Y. Leino, O. Ovaskainen and J. Piila (1995), 'Shell deformation states and the finite element method: a benchmark study of cylindrical shells', *Comput. Methods Appl. Mech. Eng.* **128**, 81–121.

J. Pitkäranta, A. M. Matache and C. Schwab (1999), Fourier mode analysis of layers in shallow shell deformations, Research Report SAM 99-18, ETH Zürich. To appear in *Comput. Methods Appl. Mech. Eng.*

E. Reissner (1945), 'The effect of transverse shear deformation on the bending of elastic plates', *J. Appl. Mech.* **67**, A69–A77.

J. Sanchez-Hubert and E. Sanchez-Palencia (1997), *Coques Elastiques Minces: Propriétés Asymptotiques*, Masson, Paris.

E. Sanchez-Palencia (1989*a*), 'Statique et dynamique des coques minces, I: Cas de flexion pure non inhibée', *C. R. Acad. Sci. Paris, Sér. I* **309**, 411–417.

E. Sanchez-Palencia (1989*b*), 'Statique et dynamique des coques minces, II: Cas de flexion pure inhibée: Approximation membranaire', *C. R. Acad. Sci. Paris, Sér. I* **309**, 531–537.

E. Sanchez-Palencia (1992), 'Asymptotic and spectral properties of a class of singular-stiff problems', *J. Math. Pures Appl.* **71**, 379–406.

https://doi.org/10.1017/S0962492901000034 Published online by Cambridge University Press